Estimating tree groundwater transpiration in La Mata catchment (Spain)

Benjamin Asigbui Agbakpe
February, 2009

Estimating tree groundwater transpiration in La Mata catchment (Spain)

by

Benjamin Asigbui Agbakpe

Thesis submitted to the International Institute for Geo-information Science and Earth Observation in partial fulfilment of the requirements for the degree of Master of Science in Geo-information Science and Earth Observation, Specialisation: Water Resources and Environmental Management

Thesis Assessment Board

Chairman:	Prof. Dr. Z. Su
External examiner :	Dr. Ir. C.M.J. Jacobs
Supervisor :	Dr. Ir. M.W. Lubczynski
2nd Supervisor :	Ir. G.N. Parodi
Advisor :	MSc. J.L. Reyes Acosta

INTERNATIONAL INSTITUTE FOR GEO-INFORMATION SCIENCE AND EARTH OBSERVATION
ENSCHEDE, THE NETHERLANDS

Disclaimer

This document describes work undertaken as part of a programme of study at the International Institute for Geo-information Science and Earth Observation. All views and opinions expressed therein remain the sole responsibility of the author, and do not necessarily represent those of the institute.

To Joyce Tudzi

Abstract

Understanding of vegetation activity in an ecological setting provides insight on water balance prediction of a catchment. This study focuses on groundwater sources of tree transpiration because this issue is vital in catchment groundwater balances. Multiple approaches were used to determine and analyze groundwater transpiration in La Mata Catchment of Sardon Watershed. Stable isotope tracing, soil matric potential and sap flow measurements were combined to determine contributions of saturated and unsaturated zone in the tree transpiration. The sap flux density was monitored using two methods (TDP and HFD) for the whole of the dry season making it possible to determine the dynamics of the transpiration process in the catchment. Whilst TDP was used to monitor stem circumferential and axial variation in sap flux density the HFD was used to monitor radial variations of sap flux density with sap wood depth.

The mean daily canopy transpiration determined for the dry season 2009 was 1.46 mm/day for *Q.i.* and 1.03 mm/day for *Q.p.* The transpiration was upscaled using biometric upscaling functions based on the biometric data collected within the study period. For partitioning of the sap flow measured at the tree stems, groundwater was enriched by deuterium isotope and consequently the deuterium was analyzed in groundwater, in moisture along the soil profiles and in the stem water. Two compartment mixing model based on analyses of the results of soil matric potential was used to analyze the deuterium data in establishing the sources of the water used in the transpiration process. The result showed 69% and 76% water uptake from the groundwater by *Quercus ilex* and *Quercus pyrenaica* respectively. The total transpiration was partitioned into groundwater transpiration T_g and unsaturated zone transpiration T_u based on the contribution from each zones established through the deuterium isotope analysis. The mean transpiration based on the 50x50m grid is 0.016 mm/day with 0.014mm/day and 0.002 mm/day from Tg and Tu.

Keywords: Transpiration, Soil Matric Potential, Stable Isotopes, Mixing model, Source Partitioning

Acknowledgements

I extend my heartfelt gratitude to the Netherlands Fellowship Programme for granting me the opportunity to undertake this knowledge enriching program. In the same element, my thanks go to the Ghana Irrigation Development Authority for granting me leave to undertake this study.

I am particular glad for my supervisors Dr. Ir. M.W. Lubczynski, MSc. Ir. G.N. Parodi and also for Leornado Reyes Acosta and Alain Pascal for their guidance all this while especially during the research period. I am deeply indebted to you all.

I reserve much gratitude to my field work teammates Andrea, Abubekar, Ermias, Donald, Andres, Firas and Tadese for the time we spent together in Salamanca, Spain and also in the cluster.

Thanks to all ITC staffs particularly Ir. Arno van Lieshout, Dr. J. B. Boudewijn de Smeth and Christian van de Tol for their supports. I could not forget the immense contribution of Dr. A. Gieske who has been a father unto me here in ITC.

Undoubtedly, I owe Dr. Hoori Ajami greatly for his contribution had been very great as he did not hesitate in making available to me RIP-ET and RIPGIS-NET software and other documentations for my work.

Much thanks to Prof. Jose Martinez Fernandez and staff of CIALE Institute, University of Salamanca, Spain for allowing access to their laboratory.

Final I extend my special thanks to Joyce Tudzi, Johnson Besah Agbakpe, Prosper, Mary, Florence Saviour, Simon and Emefa for their support and direction not forgetting my grandfather Godfred Asigbui Tudzi of blessed memory.

Akpe

Table of contents

List of figures

List of tables

Abbreviations

Q_s	sap flow	cm^3/h
v	sap flux density	$cm^3/cm^2/h$
r	bark thickness	cm
x	sapwood depth	cm
A_x	sapwood area	cm^2
C_c	canopy coverage	cm
dT	temperature difference	°C
dT_{max}	maximum temperature difference	°C
T	stand transpiration	cm^3/h
T_t	total tree transpiration	cm^3/h
T_u	transpiration from unsaturated zone	cm^3/h
T_g	transpiration from groundwater	cm^3/h
dT_{as}	asymmetric temperature difference	°C
dT_{sym}	symmetric temperature differences	°C
T_i	transpiration for ilex	cm^3/h
T_p	transpiration for pyrenaica	cm^3/h
T_{ci}	transpiration rate for ilex	mm/d
T_{cp}	transpiration rate for pyrenaica	mm/d
T_c	average transpiration rate	mm/d
A_c	canopy area	m^2
A_{ci}	canopy areas of ilex retrieved from the images	m^2
A_{cp}	canopy areas of pyrenaica retrieved from the images	m^2
v_i	sap flux density for ilex	$cm^3/cm^2/h$
v_p	sap flux density for pyrenaica	$cm^3/cm^2/h$
K	K-value	°C
D	diffusivity of fresh wood	cm^2/s
z_{ax}	axial distance	m
z_{tg}`	tangential distance	m
L_{sw}	length of sapwood	m
DBH	diameter at breast height	m
ET	evapotranspiration	mm/day
ET_s	surface evapotranspiration	mm/day
ET_{ss}	subsurface evapotranspiration	mm/day
ET_g	groundwater evapotranspiration	mm/day
ET_u	unsaturated zone evapotranspiration	mm/day
R	recharge	mm/day
WLE	water limited environment	
HFD	heat field deformation	
TDP	thermal dissipation probe	
V-SMOW	international Vienna Standard Mean Ocean Water	
BUF	biometric upscaling function	
Q.i.	*Quercus ilex*	

Q.p.	*Quercus pyrenaica*
NTG	natural thermal gradient
m.a.g.l.	meter above ground level
m.a.s.l.	meter above sea level
m.b.g.s	meter below ground surface
f_g	fraction of contribution from groundwater
f_u	fraction of contribution from unsaturated zone

As the steel is harden by fire and water so shall it be that out there, the sun and the rain will beat you not for your destruction but for your good.

1. Introduction and scientific background

There is an increase in water demand all over the world as population and water use per capita continue to rise putting pressure on available resources and many areas will be experiencing water scarcity(Teixeira, 2008). The water scarcity situation is threatening also due to continuous contamination of water sources (Teixeira, 2008).

Understanding of the groundwater-ecosystem relation is very important in managing groundwater resources. Tree plays an active role in water use that affects the water balance (Hernández-Santana et al., 2008; Smith and Allen, 1996). Further it is noted that tree groundwater use in water limited environments (WLE) constitutes a substantial component of the transpiration flux (Dawson, 1996). This relate to how trees adopt water uptake strategies to survive drought in WLE by developing deep root structure taking water directly from the phreatic system and capillary fringe (Lubczynski, 2009).

Groundwater according to Fetter (2001) hold more than 98% of the fresh water resource of the world. Since the groundwater is the hub of freshwater reserve for human activities and ecological systems, its proper management is very crucial. Especially in the WLE where annual rainfall is lower than annual potential evapotranspiration (Lubczynski, 2009; Simmers, 2003) the groundwater resources management becomes inevitable.

In the WLE, groundwater is the main source of water for industrial, domestic, agriculture and ecosystem support (Mapanda, 2003). This leads to competition among various groups of users which can result in over exploitation and pollution. The consequence of over exploitation leads to declining depth to water table (Dongmei et al., 2004). As a result, the ecohydrological system is affected. Pollution of groundwater sources also affects human and ecological functions of the ecosystem (International Water Law Project, 1989). The declining water table and pollution lead to loss of natural habitats, as vegetation and other dependent organism die out of water stress and pollution. Catchments are interconnected systems and for that matter, any effect in one catchment affect people and influences ecosystems (FAO, 1995; Gourbesville, 2008b).

In order to protect and conserve the groundwater resource for the benefit of human and supporting the ecosystem, there should be proper assessment, allocation and monitoring. The study of the groundwater is important to understand the interdependence of groundwater system and the vegetation (Snyder and Williams, 2000). Hence, the necessity of plans and management programs to use groundwater systems in such a way not to deprive any section of the resource and keep the ecosystem in balance. Groundwater monitoring is very important for policy formulation, planning and implementation of effective management programs and conservation of the resources. The use of hydrological models helps in better monitoring and hence understanding of the hydrological system. Utilizing groundwater models in the monitoring and management of these water resources call for accurate estimates of catchment boundary conditions. Evapotranspiration (ET) is one of the spatio-temporally variable fluxes linked to atmospheric processes and is typically difficult to estimate with

certainty. However, it is a key factors in the catchment water balance (Baird and Maddock III, 2005; Jin, 2009)

The role of vegetation is very important in the vertical soil-water profile and functioning of the ecosystem and plays a crucial role in the complex hydrological cycle studies (Dawson et al., 2002; Lambs and Berthelot, 2002; Miller, 2009; Wullschleger and Norby, 2001). The tree root system withdrawal of soil water is responsible for transpiration leading to plant growth. The spatio-temporal dynamics in soil moisture availability is critical in determining the vegetation and ecosystem structure present in an area (Lubczynski, 2009). Therefore, the management and sustenance of vegetation in water limited environments is dependent on the plants access to soil moisture and groundwater resources available.

1.1. Problem statement

Whilst groundwater constitutes a key component in the hydrological dynamics of water limited ecosystems (Lubczynski, 2009), the amount of groundwater contribution to the transpiration process in La Mata catchment is unknown. Hence it is significant to measure the availability of groundwater resources and the plants ability to acquire them for transpiration in the catchment (Burgess et al., 2000b). It is envisaged that evaluation of the contribution from groundwater sources to the transpiration process will enhance the understanding of the role that groundwater plays in the transpiration process, essentially boosting ecohydrological management.

One of the variables that determines species composition of an ecosystem is groundwater depth (Ridolfi et al., 2006). The importance of groundwater in ecohydrological management is linked to the dependence of plants on groundwater when other water sources are depleted or overtaken. In essence, groundwater depletion threatens many water-limited ecosystems where reduction and loss of vegetation is as a result of groundwater decline (Lambs et al., 2002; Stromberg et al., 1996).

Groundwater level fluctuation has a repercussion on transpiration which is linked to the groundwater balance (Baird and Maddock III, 2005; Stromberg et al., 1996). For this reason, a good estimation in terms of magnitude of the contribution of groundwater to the transpiration process, especially in the dry season, is worthy of study in order to understand the role of groundwater transpiration in groundwater balance.

1.2. Main objective

Main objective

To quantify dry season tree transpiration and groundwater transpiration in La Mata Catchment in Spain

1.2.1. Specific objectives

a) To analyze the radial and circumferential variability of sap flux in *Quercus pyrenaica* (*Q.p.*) and *Quercus ilex* (*Q.i.*)
b) To estimate total daily tree transpiration of single trees (T_t) for *Q.p.* and *Q.i.*
c) To map the tree transpiration T in the La Mata catchment

d) To partition the transpiration (T_t) into groundwater transpiration T_g and unsaturated zone transpiration T_u

e) To map groundwater transpiration T_g in La Mata catchment

1.3. Research questions

Main research question:

What is the role of groundwater transpiration in the total tree transpiration in La Mata Catchment in Spain?

Specific research questions:

a) What is the radial and circumferential variability of sap flux density in *Q.p.* and *Q.i.* species?
b) What is the mean daily volume of water transpired by each tree species?
c) What is the spatial variability of tree transpiration T in the La Mata catchment?
d) How can isotope tracing and soil matric potential be used to partition the individual tree transpiration (T_t) into T_u and T_g?
e) How can T_g be upscaled in the La Mata catchment?

1.4. Hypotheses

The following hypotheses were formulated in order to meet the above set of objectives:

1. The contributions of water sources of tree transpiration of *Q.p.* and *Q.i.* can be determined by deuterium groundwater enrichment, stem sap flow measurements and subsequent deuterium measurements of groundwater, soil and sap flow.

1.5. Assumptions

The following assumptions were made in order to apply the methods adequately:

1. There is no isotope fractionation during root water uptake of plants.
2. Groundwater recharge (R) in dry season is zero.

2. Study area

2.1. Location

La Mata catchment is part of the Sardon catchment in the Province of Salamanca in Central Western Spain in Figure 1. The study area lies on the coordinates of 738900W longitudes and 4553700 N latitudes of datum ED 1950 UTM zone 29. The Sardon catchment is the lower part of the Rio Tormes catchment within the Iberian Peninsula. Extensive work on this catchment had been done by water resource department of ITC. It is a water-limited environment with low human activity.

The area is about 4km from the Ledesma Highway and it is connected by feeder road from Trabadillo to the highway.

This study focused on La Mata area within the main Sardon catchment at the northern section close to the outlet of the Sardon River. It forms part of the discharge zone of the Sardon catchment bounded at the west by the Sardon River and in the other directions by the watershed boundary, ~ 4.1km^2 size in area.

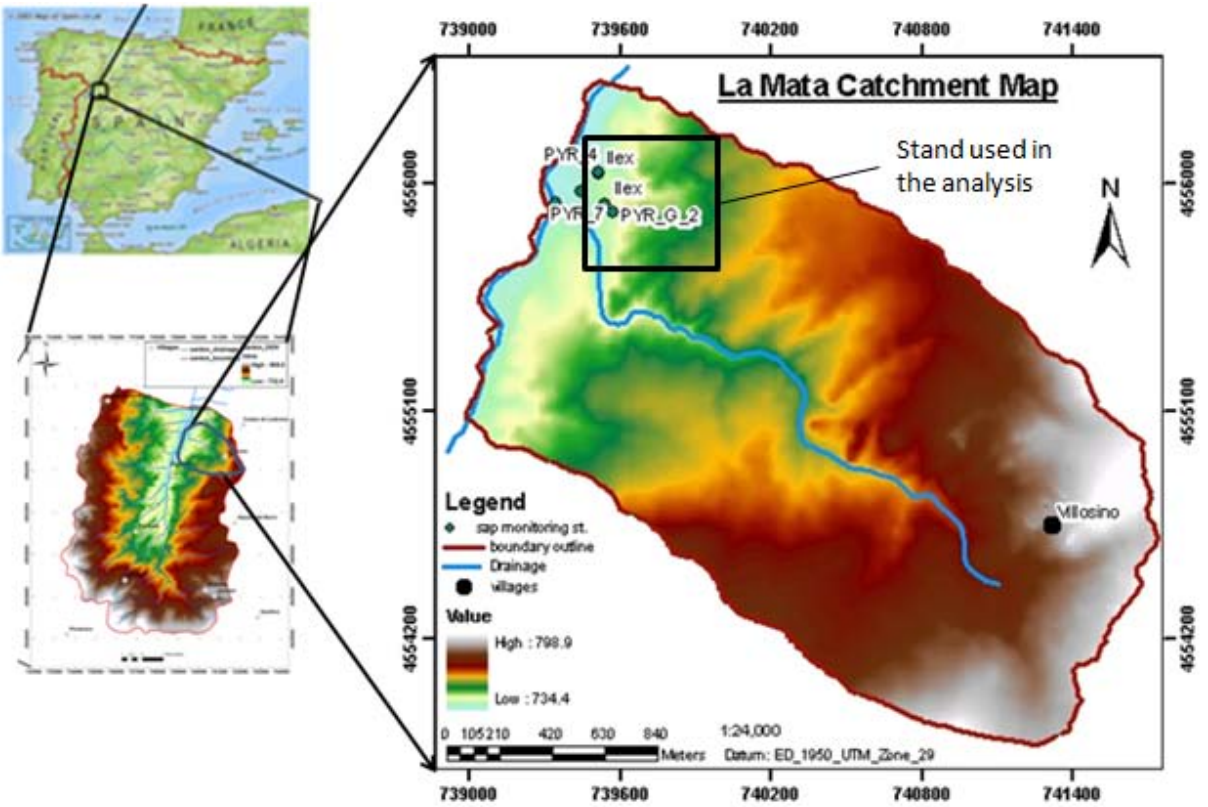

Figure 1: La Mata Catchment

2.2. Previous studies

La Mata catchment as part of Sardon catchment, has been studied intensively in the fields of geology, hydrology and ecohydrology through data integration of various measurements.

> "*The data sources and methods included: remote sensing solution of surface energy balance using satellite data, sap flow measurements, chloride mass balance, automated monitoring of climate, depth to groundwater table and river discharges, 1D reservoir modeling, GIS modeling, field cartography and aerial photo interpretation, slug and pumping tests, resistivity, electromagnetic and magnetic resonance soundings*" (Lubczynski and Gurwin, 2005).

Lubczynski and Gurwin (2005) in their study using transient model for the period spanning 1996 – 2000, arrived at the groundwater recharge of 0.3 – 0.5mm/day in the wet season whilst the dry season at no recharge. In the same study, the groundwater evapotranspiration, consisting of groundwater transpiration and groundwater evaporation, was reported for the dry season as 0.55 – 0.80mm/day and less than 0.05 mm/day in the wet season. The geological structure and characterization of the granitic basement were completed in the study of Attanayake (1999) and (Tesfai, 2001). In his study Attanayake (1999) reported of two major lithological units in the area namely megacrystic granite and peraluminous granitic rocks.

2.2.1. Geomorphology and topography

Most of the Sardon area has a gentle undulating type of topology characterized by alternating ridges and valleys. The topography is such that the southern portion is relatively steep with the middle portion flat and low-lying with the area west of the river having more gentle topography. The major drainage channel in the central part of the catchment has the lowest elevation with other tributaries also low-lying. The altitudes vary from 840m a.s.l. (at sea level) to 730 m a.s.l. from the southern section to the northern part respectively (Shakya, 2001). In La Mata catchment the land surface slope ranges from 0% minimum to 33% maximum. The low lying areas mostly along the river channel have slopes in the range of 16-33% whilst the high altitudes around the catchment boundary are almost flat. The significance of this is related to erosion.

Shakya (2001) indicated that the area is characterized by poor drainage system. Erosion is mainly caused by streams resulting in valleys and depressions which are the wetter parts in the catchment.

In the Mata area, the western boundary lies along the Sardon River in the central valley of Sardon area which constitutes the low areas and the south-eastern boundary forms the upland areas.

The area is marked by outcropping of massive non-fractured rocks. The valleys along the river banks are made of thick deposits of alluvial and colluvial materials(Lubczynski and Gurwin, 2005)

2.2.2. Climate and hydrology

The study area is characterized by low precipitation (average 20 mm/month) and high temperatures (average 22°C) during the summer with very high potential evapotranspiration (5mm/day), (Lubczynski and Gurwin, 2005) typical of water limit environments (WLE) (Cubera and Moreno, 2007; Simmers, 2003). Mostly the high precipitation period is very short and is in November to December with the precipitation figures above 100 mm/month. The mean annual precipitation record

of 23 years for six stations of Spanish Meteorological Institute was 500mm/yr and the mean monthly precipitation less than 20mm/month (Lubczynski and Gurwin, 2005).

Usually, the warmest months are August-September with daily temperatures going above 35 °C and the average monthly summer temperature about 22 °C. The low temperatures are recorded in the month of January – February with average monthly winter temperature around 5 °C. The potential evapotranspiration is very high exceeding the annual rainfall with the average value of 5 mm/d (Lubczynski and Gurwin, 2005).

La Mata stream drains into the Sardon River which flows into the Rio Tormes River. Apart from La Mata stream, there are many other networks of streams in the area, which are drained into the Sardon River. The peak flow of the river is in April – May and November – January (Shakya, 2001). The Sardon River mostly dries up from middle of June to middle of October (Shakya, 2001). The Sardon River is noted to recharge quickly during the rainy season due to high runoff process aided by low retention capacity of the highly permeable unconsolidated top layer (Shakya, 2001). During high intensity rainfall, the direct runoff process is high both in the surface and the subsurface.

The presence of fractures, gentle slope of terrain and the weathered layers in the valley and loose alluvial material promotes infiltration nonetheless much of the rain water evaporates or flows out (Shakya, 2001).

2.2.3. Geology and soil

The Sardon catchment forms part of the Iberian massif which is underlain by granitic rocks with quartz dykes intrusions. Shakya (2001) reported granite weathering characterized by deep weathering in the valleys and outcrops in the hilltops in the Sardon Catchment (refer to Figure 3).
The geological study carried out in the Sardon area by Attanayake (1999) categorized the lithological units into two: mainly peraluminous leucogranitic and megacrystic granite based on Salamanca-Zamora regional lithological unit. The two-mica granite forms 70% and the megacrystic granite forms 15% of the area.
The geology is made of schist and granites at the south and granites at the western and the northern part whilst the eastern part is mainly quartzite filled fractures.

2.2.4. Vegetation and land use

The vegetation of the La Mata area is composed of natural vegetation, dominated by *Quercus ilex* and *Quercus pyrenaica* tree species. The *Quercus pyrenaica* also locally known as melojo oak, is an indigenous species in the Iberian Peninsula. The *Quercus pyrenaica* leaves have smooth margin that are lobed and 10-15cm length, besides they do not easily fall even in severe conditions (Wikipedia, 2009 -b). The acorns produce by the tree is oblong in shape and measure about 1.5-3cm. (Exploring the World of Trees, 2009 (access yr)). The *Quercus pyrenaica* is known to have a dense root system up to 60cm and a tap root system reaching deep into the soil for exploring deep layer soil water and shallow groundwater to survive summer water deficits (Hernández-Santana et al., 2008; Lubczynski and Gurwin, 2005; Silva et al., 2003; Silva and Rego, 2004).

The *Quercus ilex* also known as Holm Oak and locally as encina oak, is a medium to large tree depending on the growing condition and it is indigenous to the Mediterranean region. The mature trees usually grow to a height of 20-27m and multiple branches round crown (Wikipedia, 2009 -a). Mostly, Quercus ilex is noted for forming cluster forest in the sub-humid regions though grows well in all bio-climates (Brereton et al., 2009). This species is known to survive harsh climatic and soil conditions but slow rate of growth. It has evergreen foliage; leaves are leathery, dark green above and grayish beneath and of variable shape which lose their spikes as they grow older (Wikipedia, 2009 -a). The mature leaves are 4-8 cm long and 1-3 cm broad having short hairs beneath and it is in leave all year round. The leaves take 1-2 years to fall after new ones are formed. The bark of the tree is blackish with fine square-fissures (Brereton et al., 2009). The *Q.i.* tree flowers in May – June and bear acorns in September – October which is about 2cm long which takes 6months to mature and are bitter testing. The acorn is green when young but reddish brown when it is ripped. The acorns are edible and serve as source of food for Serrano ham (Ontiveros, 2009).

The canopy area covers 19% of the study area with *Q.i.* covering 12% whilst *Q.p.* covers 7% of the area the rest of the area is composed of shrubs and grass. Natural woody-shrubs dominated by *Cyticus scoparicus* locally known as escobar or Scotch Broom sparsely dot the area with grass and weeds typical of water limited environments available making the area viable for livestock production (Shakya, 2001). Cyticus scoparicus is noted for invasion by spreading to the territories of grasses and young trees to form a pure stand (Lubczynski and Gurwin, 2005).

Crop production activities are limited in the area as the topsoil is shallow. Irrigated agriculture is carried out at the upper catchment close to the watershed boundary of La Mata.

2.2.5. Hydrogeology

The granitic composition of the area generally controls the hydrogeology of the catchment (Lubczynski and Gurwin, 2005). The weathering and fracturing processes plays a major role on the hydrogeology of the catchment.

In addition the fault system (Figure 2 & Figure 3) in the study area influences both the regional and the local hydrogeological flow system (Uria Cornejo, 2000). The depth to water table in the area is shallow in the valley varying from (0-3) m to about 5m at the upper limits of the catchment (Shakya, 2001). The groundwater flow regime is towards the fault drainage line lying along the Sardon stream. Weathering and fracturing of the granitic basement rock influence the hydrogeology of the area. Consequently, three layers had been reported in this area made of weathered granitic rocks at the top, fractured granitic rocks and alluvial deposits and massive impermeable rocks at few meters to about 60 m b.g.s (Attanayake, 1999).

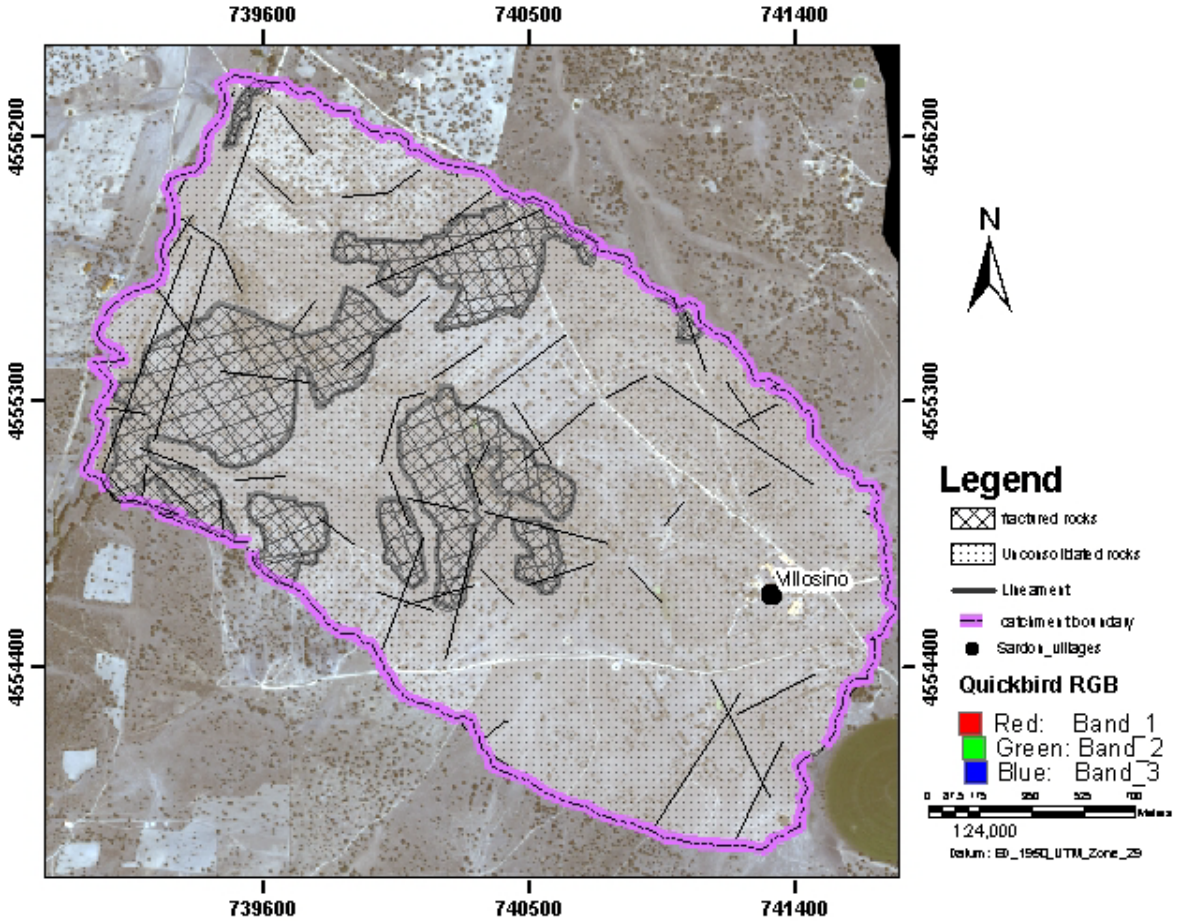

Figure 2: Surface geological formation of La Mata catchment after Shakya (2001)

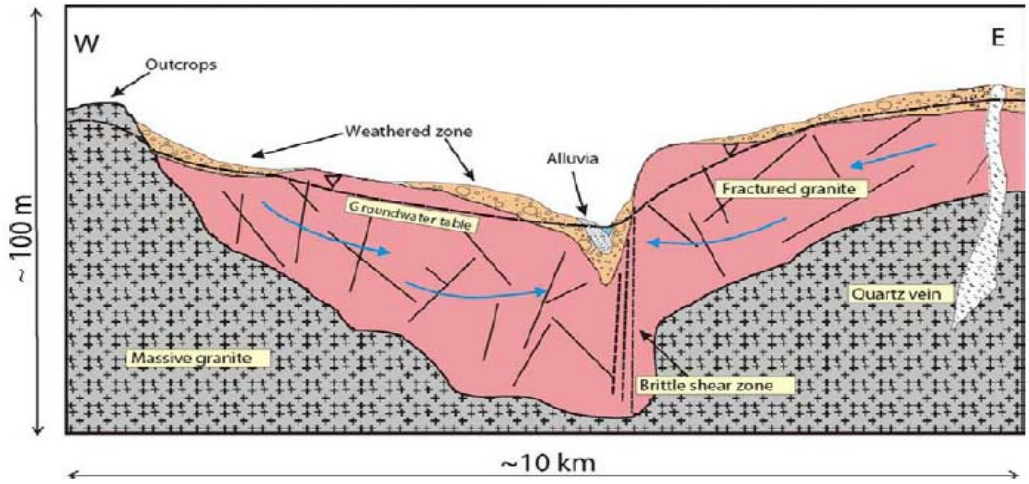

Figure 3: Schematic cross-section of geological formations in Sardon catchment (Fig. 1) after Lubczynski and Gurwin (2005)

3. Materials and Method

3.1. Materials and Equipments

The materials used for data acquisition during the field campaign include the following: Cobra corer, sap extractor, portable fridge (cooler), suction pump, Garmin GPS (Garmin International), Granier Sap Sensor (Dynamax Lincoln, NE), HFD Sap Sensor (ICT), Delta-T Data logger (Delta-T Devices Ltd) and Campbell Data logger (Campbell Scientific USA).

3.2. Methods

The outline of the research process is as shown in the flowchart in Figure 4.

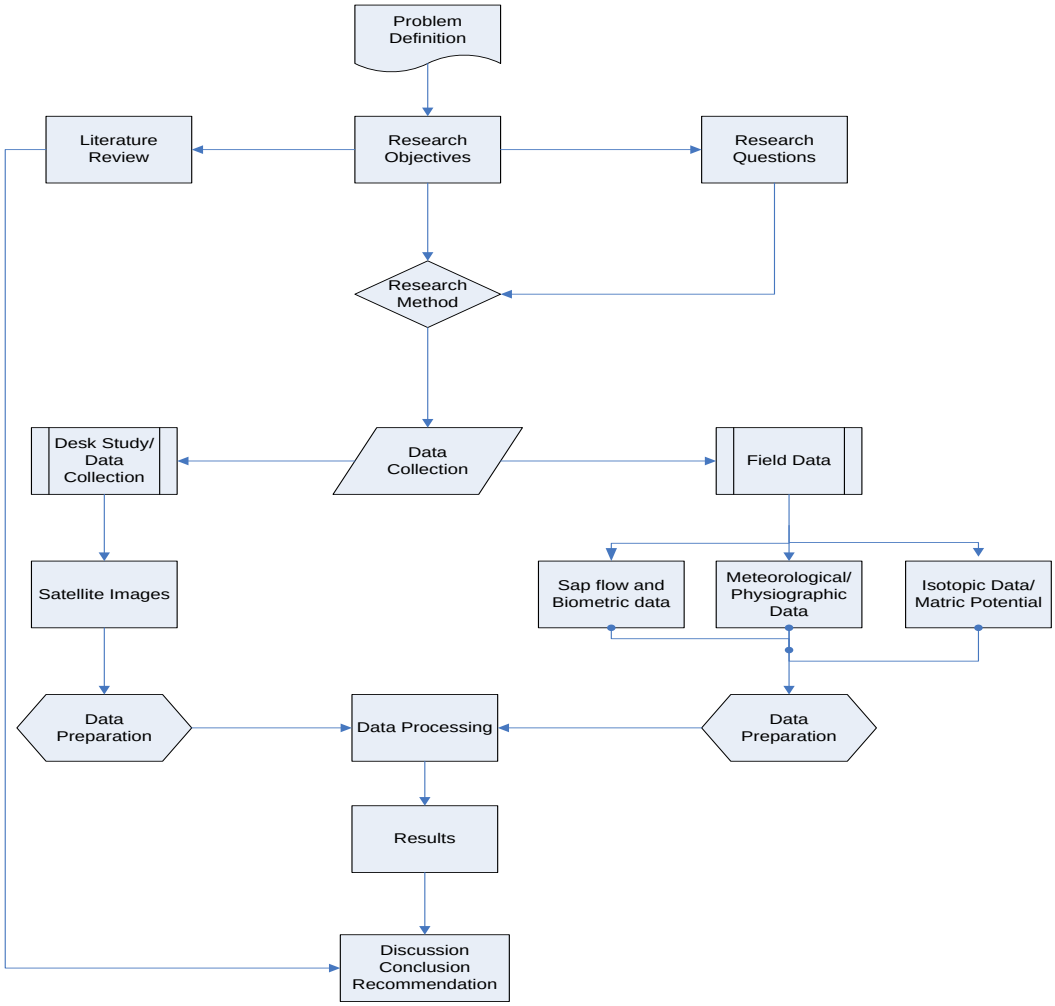

Figure 4: Flow chart of the research process

The research process runs through problem definition, objectives and questions with literature support leading to the methods and the data requirements to achieve the objectives Figure 4. These processes lead to the data processing, results, discussion, conclusion and recommendation

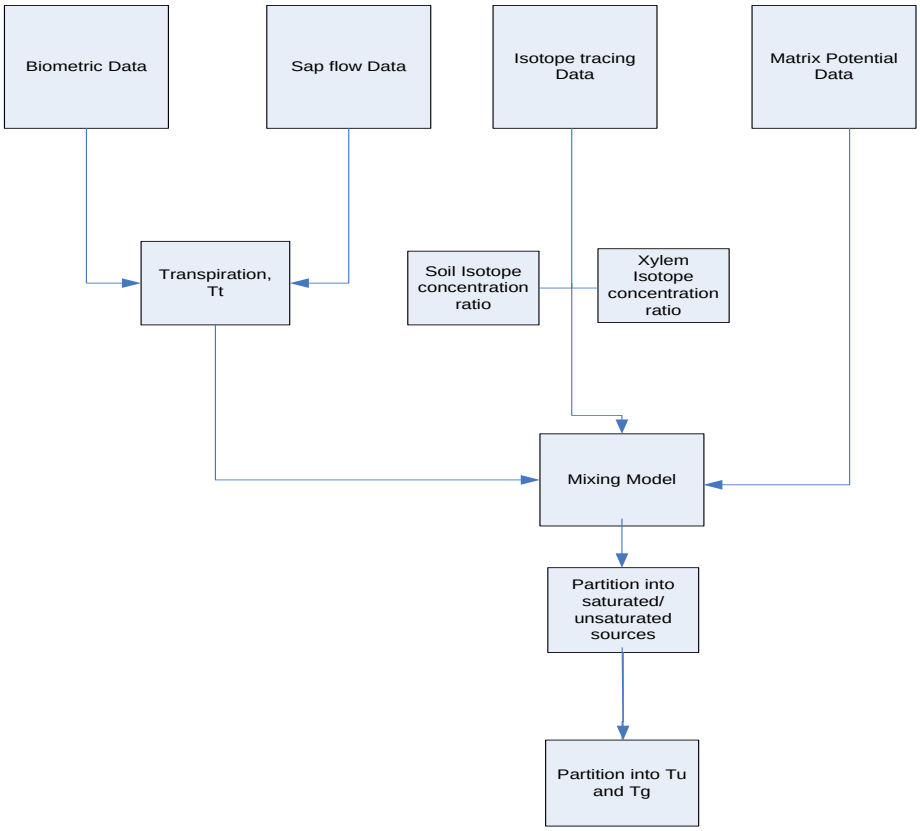

Figure 5: Flow chart on method and steps

In order to define and quantify the tree groundwater uptake mechanisms, two methods have been combined. These methods are: sap flow monitoring, and stable isotopes tracing combined with soil matric potential. The methods and steps are enumerated in Figure 5.

This involved sap flow measurements in addition to biometric data collection which were used to estimate the transpiration (refer to Figure 5). The soil matrix potential measurement is to identify the depth in which water is available in the soil profile for the plants and combining this with stable isotope measurements to discretize the zones where the plants source water for the transpiration. Consequently applying source partitioning mixing model, the fractional contribution from each zones were estimated as detailed in subsequent sections.

3.2.1. Sap flow monitoring

There are various approaches in assessing tree transpiration. These approaches are based on thermodynamic, electric, magneto-hydrodynamic and nuclear magnetic resonance (Čermák et al., 2004).

In this research, the heat field deformation (HFD) method (Nadezdina,1991) quoted by Cermak et al (2004) is used in addition to the thermal dissipation method (Granier, 1985).

TDP

Thermal dissipation method effectively determines the occurrence of sap flow in the xylem and estimates its velocity (Ziegler et al., 2009) also know as sap flux density. It is based on comparison of temperature between two probes radially inserted into the xylem (Burgess et al., 2000a; Smith and Allen, 1996). The TDP probes use two cylindrical thermocouples for measuring the temperature. The upper probe is heated whilst the lower is at the ambient temperature of the tree. The thermocouples thus measure the temperature difference between the two probes (refer to Figure 6). The sap flux density measured in the xylem with Granier-type sensors represents the flux averaged over the 2 cm sensor length (Oren et al., 1999).

If there is no change of sap storage along the stem, the tree transpiration T_t is equivalent to the sap flow Q_s, i.e. $T_t = Q_s$ and

$$Q_s = v \cdot A_x \qquad \textbf{1}$$

where Q_s is typically in cm^3/h, v is the sap flux density in $cm^3/cm^2/h$ and A_x is the sapwood area in cm^2.

Sap flux density (TDP)

The sap flux density in TDP method is derived by the following formula:

$$v = 118.99x10^{-6}\left[\frac{dT_{\max} - dT}{dT}\right]^{1.231} \qquad \textbf{2}$$

where dT_{max} is the maximum daily temperature change in °C recorded at zero flux and dT is the temperature difference °C recorded at a given velocity.

The TDP for sap flux density measurements consists of a pair of needles of 2mm diameter and 2cm long. The installations was done on a tree with well formed stem by part removal of the tree bark and drilling two axial holes with 10cm separation into the tree one above and one below at about 1.3m above the ground. In case of all other trees monitored with just one sensor, this was installed at the northern side of the tree to avoid direct solar radiations affecting the result (Lu et al., 2004; Wullschleger and King, 2000). Aluminium tubes were inserted into the drilled holes. The probes were finally wrapped in silicone gel to improve thermal conductivity and inserted into aluminium tubes.

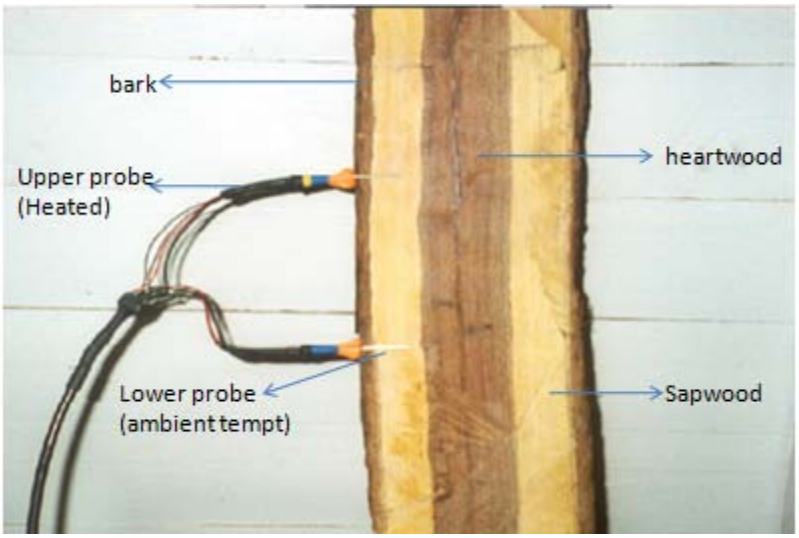

Figure 6: Typical Arrangement of TDP in a tree, source: (Mapanda, 2003)

A sunshield was used to cover the probes and it served dual purpose, as protection against direct sunray and rainfall. The TDP sensors were connected to the Campbell Data Logger which was programmed to give 30 seconds sampled of the temperature difference dT averaged and stores at 10min interval. The system was connected to 12 volt power supply source which serves as the power supply for the heater probe using 0.2W of continuous energy supply.

The sap flux density measurements field campaign started 12 June (Leonardo Reyes Acosta) and lasted till September 2009. Six pairs of TDP were used to monitor *Q.i.* and *Q.p.* each; three pairs in the north facing side, one pair in the eastern, western and southern directions recording 30s time step. In the north facing side, the first sensor was installed close to the crown at the first branch, the second one at 1.3 m a.g.l and the last one at 0.3 m a.g.l. In the other directions, the sensors were installed at 1.3 m a.g.l. It was later noted that three of the sensors in *Q.p.* were malfunctioning and were disconnected on 23 July leaving only three in the northern, southern and western directions. During the September 2009 field campaign, sap flux density was measured in additional three *Q.p.* with TDP sensors from 06/09/2009 to 13/09/2009.

The sap flux density data processing was done by first checking the consistency of the data. This was done by plotting the temperature differences (dT) for a number of days. The maximum temperature change, dT_{max} was determined for each day. The 20 min and 30 min dT were then averaged to the hourly dT for all the six TDP pairs of *Q.i.* and three TDP pairs for *Q.p.* and for the single sensor measurements done on three additional *Q.p.* The obtained sap flux densities were further aggregated into the daily averages.

Sapwood depth and sapwood area (A_x)

The sapwood is the part of xylem between the cambium and the heartwood (see Figure 9), consisting of treachery elements and parenchyma ray cell (Lu et al., 2004). The sapwood is the living area of the tree that serves as conduit for transport of water and minerals for the tree (Wullschleger and King, 2000). That is for sap flow analysis of a tree; the sapwood area needs to be estimated in other to calculate the total sap flow for a whole tree (Lu et al., 2004). The sapwood area depends on the

growing stage of a tree and is also species dependent. Sapwood area (A_x) estimate is critical in any assessment of sap flow as indicated by Equation 1.

The sapwood identification is easy in trees which form distinct heartwood with coloration such as *Q.p.* More difficult is A_x estimate in trees with heartwood not differentiated by colour; for example in *Q.i.* the younger trees do not show distinct sapwood coloration. However, according to Lu et al. (2004) heartwood coloration boundary alone is not reliable indicator of sapwood boundary. Generally, in some species, it is impossible determining the boundary between sapwood and heartwood (Lu et al., 2004).

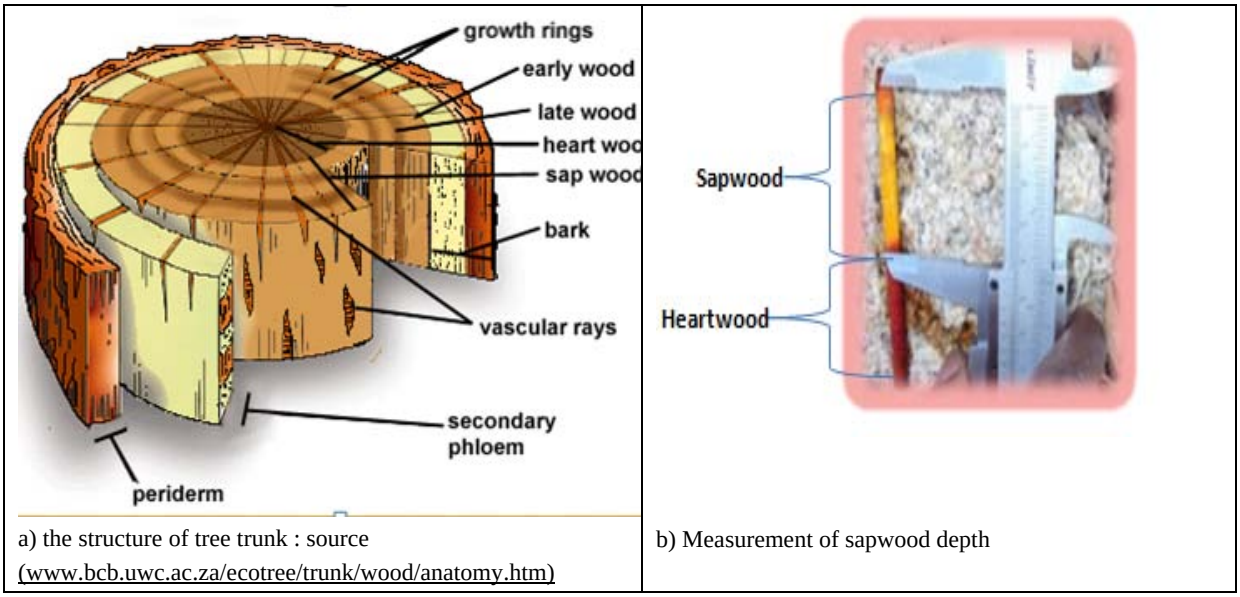

a) the structure of tree trunk : source (www.bcb.uwc.ac.za/ecotree/trunk/wood/anatomy.htm)

b) Measurement of sapwood depth

Figure 7: a) Structure of the tree stem b) measurement of sapwood depth

In this study the sapwood depth was measured by taking samples from the tree using a Presler corer. The bark of the tree (usually 1cm for *Q.i.* and 1.5cm for *Q.p.*) at breast height was chiselled out and the corer was driven into the tree by given it a right screw turn. With about 20 turns, about 10 cm of wood was taken from the tree. The sapwood section was identified by adding methyl orange to the core taken to enhance differentiation of the sapwood from the heartwood based on visual examination. A veneer caliper was then used to measure the sapwood depth Figure 9b.

The cross-sectional sapwood area was computed from the stem diameter at breast height, sapwood depth and bark depth using the relation:

$$A_x = \pi\left(\frac{D}{2} - r\right)^2 - \pi\left(\frac{D}{2} - x\right)^2 \qquad \mathbf{2}$$

Where A_x is the sapwood area in cm^2 and D is the diameter at breast height in cm, r is the bark depth in cm and x is the sapwood depth in cm.
The estimated bark radius r is 1.0 cm and 1.5 cm for *Q.i.* and *Q.p.* respectively.

HFD

In the HFD, the deformation of a heat field around a heater needle inserted radially in the stem is measured (Čermák et al., 2004; Nadezhdina et al., 2002; Nadezhdina et al., 2006). The HFD method

uses four needles of 1.5 mm diameter, which include one heater and three sensors. The heater is 110 mm length whilst the sensors are 100mm length with 8 measuring points (thermocouples). The upper and the lower sensors measure the symmetrical temperature difference (dT_{sym}) whilst the side sensor measures the asymmetrical temperature difference (dT_{as}) (ICT, 2009). Sensor arrangement is shown is Figure 7 & 8.

This method had been applied in various studies of whole tree transpiration and root water uptake and redistribution (Gartner et al., 2009; Nadezhdina et al., 2006; Nadezhdina et al., 2004) and in plant water storage (Verbeeck et al., 2007). The HFD method is good for analyzing the variability of sap flux density with sapwood depth.

The HFD method measures the temperature difference dT of the sapwood using thermodynamic technique. The dT is measured both symmetrically (in the axial direction, above and below) and asymmetrically (in the tangential direction or to the side) around a line heater (Figure 7 & 8). The heater is heated using a current of 50mA which produces an elliptical heat pattern under condition of zero flow. With sap flow, the elliptical heat field is deformed and elongated. The bidirectional flow and very low flow measurements are given by the symmetrical temperature difference (dT_{sym}). The medium to high magnitude flow rates are given by the asymmetrical temperature difference (dT_{as}) (ICT, 2009). In Figure 7 the temperature difference dT_{sym} is between the upper and the heater probe for the forward flow and between heater and lower probe for the reverse flow. The temperature difference dT_{as} is between side sensor and heater probe.

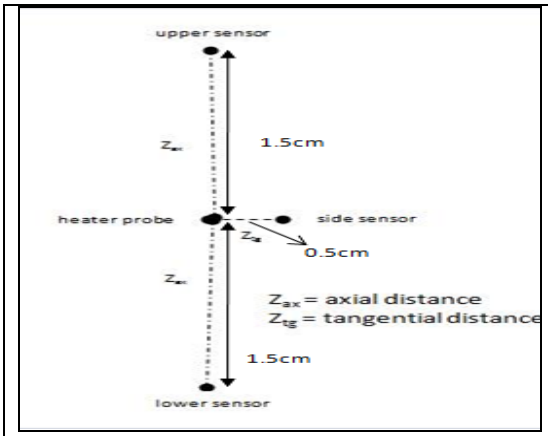

Figure 8: Schematic arrangement of HFD probes

The HFD technique uses the ratio of differentials to calculate sap flow. The equation used for the calculation is given as

$$v_i = 3600D\frac{Z_{ax}}{Z_{tg}}\frac{1}{L_{sw}}\left(\frac{K + dT_{sym} - dT_{as}}{dT_{as}}\right) \qquad 4$$

Where v_i is sap flux density in $cm^3/cm^2/h$ at position *i* and the 3600 is used to convert second to hour, D is the thermal diffusivity of fresh wood in cm^2/s, Z_{ax} is the axial distance in cm, Z_{tg} is the tangential distance in cm, L_{sw} is the sapwood depth in cm, dT_{sym} and dT_{as} are symmetric and asymmetric temperature gradients respectively, K is the absolute value of dT_{as} (ICT, 2009).

The value of dT_{sym} gives zero flow; flow direction for the positive and reverse flow conditions are calculated from temperature gradients dT_{as} and (dT_{sym}-dT_{as}) (Nadezhdina et al., 2006; Nadezhdina et al., 2008).

In the period June – September, the HFD was used to monitor sap flux density in three *Q.i.* and two *Q.p.* The measurements for *Q.i.* were done in: 23 Aug – 4 Sept, 14-18 Sept and 18 – 24 Sept and for *Q.p.* in: 24 Jul – 29 Jul and 4 Aug – 14 Aug. However the readings 18 – 24 September were not good because of logger programming problem.

Installation of HFD

The procedure followed in the installation of the HFD sensor includes partial removal of the bark of the tree and attaching the HFD jig with Velcro strap to hold it in position. Four holes were drilled slowly into the tree according to the jig starting with the lower hole then to the upper hole, followed by the side holes. The jig is to ensure a good alignment for the holes to keep the holes parallel into the tree. A sleeve in the jig was removed and the process continued until the final drilling when the drill was removed completely.

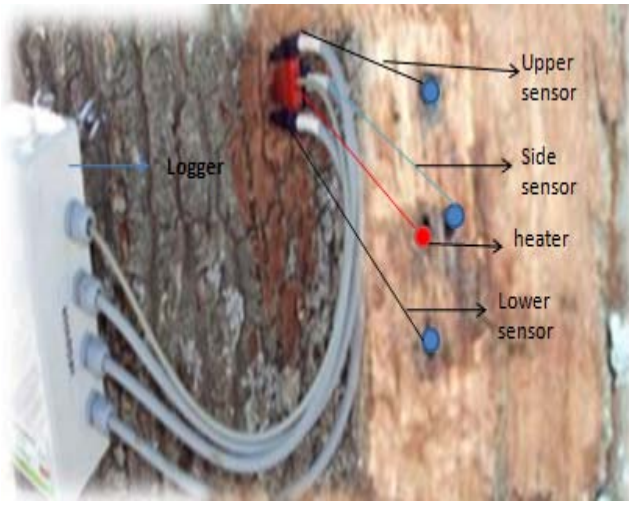

a) Typical arrangement of HFD sensors

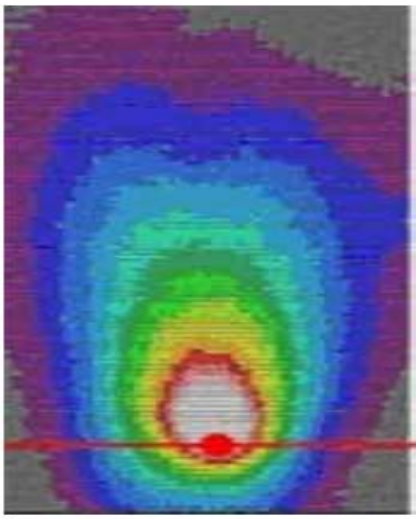

b) Elliptical deformation of heat filed (Taken from ICT Manual)

Figure 9: HFD: a) typical installation of HFD sensors; b) deformation of heat field

In every HFD installation, first an aluminium tube was inserted into each drilled hole. Next, the needles (sensor and heater) were covered in silicone gel to enhance conductivity and inserted into the aluminium tubes in the holes. Afterwards system was connected to the powers supply consisting of battery, solar panel and charge regulator. The data was controlled and downloaded from the SMART logger (ICT).

The sap flow data collected using the HFD was processed using the sap flow tool software by ICT (2009) base on Equation 4 calculating the sap flux density for each sensor. The data is checked for biased data which were removed and new values interpolated to fill the gaps.

3.2.2. Spatial representation of tree transpiration T

In upscaling, information is collated on a smaller spatial scale and integrated it to derive information at larger spatial scale (Mapanda, 2003). Upscaling can be done using two procedures: field measurement of scalars i.e. stem area that is correlated with the upscaled parameter and use of remote sensing to retrieve scalars such as canopy area (Lubczynski, 2009).

In order to access the spatial variability of tree transpiration in the study area, characteristics of the trees in the area were collected for establishing biometric relations to correlate them with sapwood area and further use them for upscalling according to biometric upscalling functions.

Biometric Data

An inventory of biometric data of both *Q.i.* and *Q.*p. was done in the La Mata catchment in order to develop allometric relations for upscaling of the sap flow measurements. The trees selected for sampling were chosen to cover various sizes of trees available in the catchment.

The parameters sampled include diameter at breast height (DBH), height at first branching (HB), Height to crown top H_t, Sapwood depth (x), and Canopy coverage (C_c). All the parameters were obtained to give a wide range description to the characteristics of the trees. All sampled trees were identified on the QuickBird image in the field and additionally their coordinates were recorded using Garmin GPS handheld receiver operating in differential mode.

Biometric Upscaling Functions

The field biometric data was analyzed using correlation analysis in which the sapwood area was correlated with the canopy area and stem area to establish a relation among them. The scalar with good correlation among them was used in defining the species dependent biometric upscaling function (BUF). The BUF is used to upscale the sap flux into the catchment.

Canopy transpiration flux rate Tc (normalized sap flow)

The canopy flux rate is computed based on the relation

$$T_c = \frac{v.A_x}{A_c} \qquad \textbf{3}$$

Where T_c is the canopy flow rate in cm/h, v is sap flux density in $cm^3/cm^2/h$, A_x is sapwood area in cm^2 and canopy area A_c in cm^2.

Stand transpiration and catchment transpiration

The stand transpiration is

$$T_s = \frac{\sum_{i=1}^{n} v_{Q.i-i}.A_{xQ.i-i} + \sum_{i=1}^{n} v_{Q.p_{-i}}.A_{xQ.p-i}}{A_{st}} \qquad 7$$

Where T_s is the stand transpiration cm/h, $v_{Q.i.-i}$ and $v_{Q.p-i}$ sap flux density in $cm^3/cm^2/h$ of *Q.i.* and Q.p., $A_{xQ.i-i}$ and $A_{xQ.p-i}$, sapwood area cm^2, A_{st} stand area in cm^2 and n is number of trees in the stand.

The catchment transpiration is

$$T_{ca} = \frac{\sum_{i=1}^{n} v_{Q.i_i} . A_{xQ.i_i} + \sum_{i=1}^{n} v_{Q.p_i} . A_{xQ.p_i}}{A_{ca}} \qquad 8$$

Where T_{ca} is the stand transpiration cm/h, $v_{Q.i.-i}$ and $v_{Q.p-i}$ sap flux density in $cm^3/cm^2/h$ of *Q.i.*, $A_{xQ.i-i}$ and $A_{xQ.p-i}$, sapwood area cm^2, A_{ca} catchment area in cm^2 and n is number of trees in the catchment

3.2.3. Soil Matric Potential Measurement

An important variable in determining water availability to plants is soil matric potential (González, 2001). In order to extract water retained in the soil, plant roots have to overcome the force by which water is held in the soil. Above a certain threshold (wilting point), the plants are unable to extract water from the soil. In this study it is assumed that zones with matric potential greater than -1.0MPa are an adequate water source for the plant (Walker et al., 2001). It is therefore important to know the matric potential of the soil in determining the zones from which plants source their water. The matric potential therefore complements other data sources in ascertaining the zones from which plants source their water.

Soil matric potential representative of the layers under natural conditions were determined in profile at four different depths of the soil. The idea was to determine a representative value of the soil matric potential without sample variations in the moisture content of the soil.

Three different locations were used as sampling points: under the canopy of a *Q.p.*, a *Q.i.* and in a bare soil area. In the location around the *Q.p.* and *Q.i.* the samples were taken along north-south transects (Figure 11). The first point in the transect was located half the radius of the tree canopy and the second at the edge of the canopy. The third point was out of the area of the canopy of the tree in both directions. The sampling was carried out using 10cm diameter hand auger at the depths of 25cm, 50cm, 75cm and 100cm at each point. The samples were taken and kept under sealed and frozen to minimize evaporation from the sample.

The soil matric potential was measured in the lab using a WP4 device (Decagon Devices Inc. Pullman Washington, USA) with a range of 0 to -300MPa.

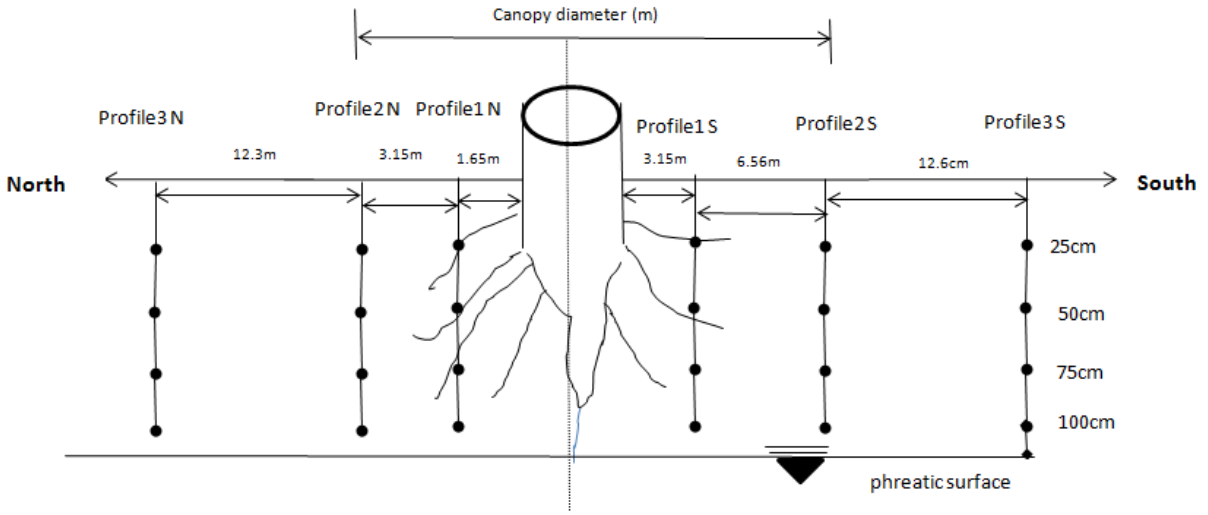

Figure 10: Diagram of the sampling transect for the soil water potential profile under the tree.

3.2.4. Stable isotope tracing

The stable isotope tracing method is applied in combination with the soil matric potential. Previous research showed that the combination of stable isotope techniques and sap flow measurements presents a powerful tool to assess groundwater use in tree species (Cramer et al., 1999). This study uses both the natural abundance isotope data and deuterium enrichment.

The (^{2}H and ^{18}O) are naturally occurring stable isotopes which are abundant in the soil. These stable isotopes had been used as non-radioactive tracers and non-destructive integrators of ecohydrological interaction. Within the past decade the use of stable isotopes to study how plants interact with groundwater had improved steadily (Dawson et al., 2002). The method had been used in identifying the various water uptake zones of plants (Burgess et al., 2000b; Schwinning et al., 2002; Thorburn et al., 1993) i.e. assessing whether trees use groundwater during the dry season or not (Lamontagne et al., 2005).

Under the applied tracer method, the assumption is that the isotopic composition of the source does not change as it is extracted by the plant. For this reason, if the plant obtained all its water from a common source, the isotopic composition of the plant water and the source water should be similar (Walker et al., 2001). Thus the isotopic composition should be mixture of composition from various compartments in case of use of several sources (Brunel et al., 1997).

The isotope composition is expressed as a ratio of heavy and light isotopes denoted in standard delta notation ($\delta^{2}H$) in parts per thousand (‰) relative to Vienna Standard Ocean Water (V-SMOW). The isotope ratio is express as:

$$\delta^{2}H = \left(\left(\frac{R_{sample}}{R_{V-SMOW}}\right) - 1\right).1000‰ \qquad 4$$

Where $\delta^{2}H$ is the deuterium ratio in part per thousand, R_{sample} is the ratio of heavy and light isotopes sampled and $R_{V\text{-}SMOW}$ is the standard isotope ratio.

The use of water of artificially enriched deuterium had been employed in water uptakes studies with good results. In their studies, Ehleringer and Dawson (1992), Lambs et al. (2002) and Walker et al. (2001) applied this method in the studies of water sources and uptake zones of plants.

In this study, an independent tracer of enriched deuterium composition was applied to the ground water. If plants take up groundwater, after the deuterium enrichment of groundwater, this is signified by subsequent stem sap water enrichment proportional to groundwater contribution.

The stable isotope deuterium composition before the tracer application was checked by taking samples from the soil and the xylem. The soil samples were taken from the location about 3m away from the tree trunk, at four different depths of 25cm, 50cm, 75cm and 100cm. The samples were taken using Cobra auger and samples were sealed and put in cold storage to avoid evaporation. The corresponding stable deuterium composition in the xylem was also measured by sap extraction from the cores taken from the stem using Presler corer. Seven cores were taken from the tree which gave enough quantity of extracted sap (3ml). The sap was extracted using a field sap extractor.

The sap extractor is a hydraulic press system made up of a cylindrical extraction chamber, a piston and a pressure gauge (Lambs and Berthelot, 2002). The extracted sapwoods broken into smaller pieces were put in the chamber and the top closed with the piston. This is then connected to the hydraulic press and a pressure applied manually using the handle. The maximum pressure attainable with this press was 70MPa (Lambs and Berthelot, 2002). Usually, the sap starts flowing at attainment of 20MPa and continues to flow as the pressure is increased to 65MPa.

The experiment was carried out on selected trees of *Q.i.* and *Q.p.* In the experimental setup five piezometers tapping groundwater, were installed in both locations. This was to ensure that the deuterium injected reached the water table directly an uniformly. The depth to the water table in case of the two trees monitored was about 110 m. Four of the piezometers served as injection piezometers whilst the fifth one was the monitoring piezometer. The arrangements of the piezometers were in the four cardinal points, 2m away from the tree whilst the monitoring piezometer is 1m from the tree as shown in Figure 12.

The four piezometers were injected with 30 litres of deuterium rich water (+1300 dH-2 [‰] aprox.) of 10 litres a day for three consecutive days. The injection was done using 3 mm rubber hose with a length extending into the water table with a regulator connected to 900 ml bottle. The bottles were filled with the deuterium rich water and the hose was passed through the 3.5mm hole cut in the cap used to close the top of the piezometers. The water was released into the piezometers by adjusting the regulators. The injection was done in drops in order not to induce sudden increase in the water level in the piezometers.

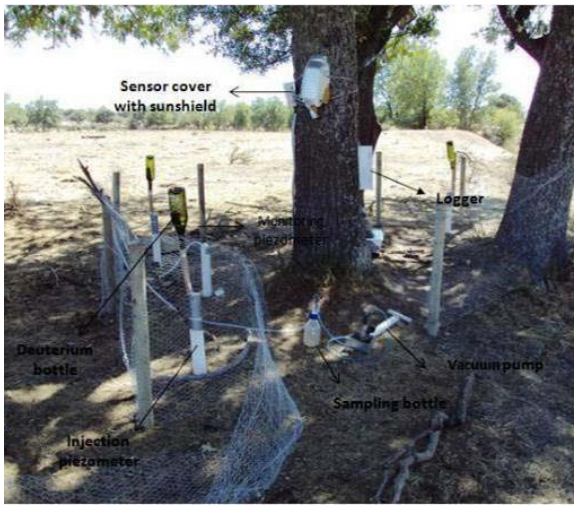

a) Picture of the deuterium test

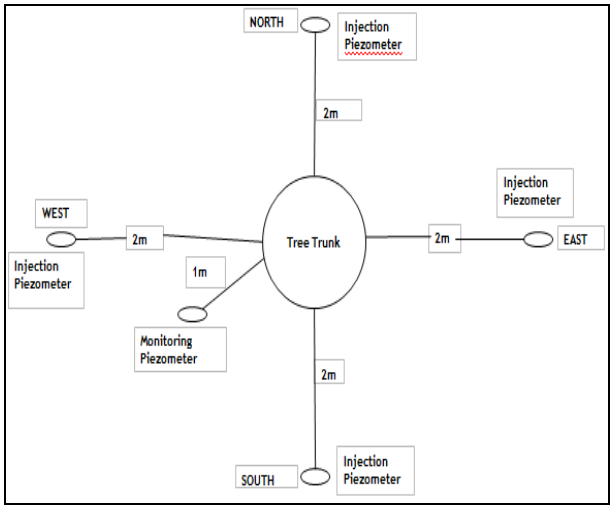

b) Sketch of the arrangement of deuterium test

Figure 11 : typical arrangement for deuterium tracer test under a tree

After completion of the third injection, 24h deuterium monitoring began. This was done by sampling water from the monitoring well using suction cups and a vacuum pump. While taking the water sample, seven sapwood samples were also taken with a Pressler corer. They were quickly put in test tubes and closed with caps and stored in a freezer to avoid evaporation. The sap from the sapwood was extracted using hydraulic press system. The extracted sap was put in a test tube sealed with paraffin and stored in the freezer on the field to avoid evaporation. The sampling process was repeated at 3h intervals for 24 h. From 9:00 pm until 8:00 am, only the groundwater was monitored as earlier data collected during the field work shows that transpiration was zero during this period. Then in the morning at sunrise the procedure continued with the sap and groundwater monitoring till 11am.

The sampling of the sap and the groundwater continued for one week on daily basis with each sample taken at 11am each day. The samples collected were then sent to the lab for analysis and determination of the deuterium signature and level of composition. The extraction of the water from the soil was done by azeotropic distillation. The deuterium analysis was done using continuous-flow isotope ratio mass spectrometry by Iso Analytical, UK laboratory.

The result of the deuterium compositions in the samples were analyzed using end-member mixing model (Snyder and Williams, 2000). Due to the stable isotopic signature of sap-water and of the saturated and unsaturated zone, the soil matric potential was used to partition various water sources. The mixing model relation (Dawson et al., 2002) is:

$$\delta_t = f_g \delta_g + (1 - f_u)\delta_u \qquad \textbf{5}$$

$$f_g = \frac{(\delta_t - \delta_u)}{(\delta_g - \delta_u)} \qquad \textbf{6}$$

Where f_g, f_u fractional contributions from the groundwater and unsaturated zones, and the δ_t, δ_g and δ_u are the isotopic ratio composition from sap-water, saturated and unsaturated zones respectively.

In estimating fractional components from each zone, it was assumed that the δ_u was invariant within the monitoring period. The mean value from the possible unsaturated zone was assigned as δ_u in computing the fractions. According to Kendall and McDonnel (1998) there should be a difference of at least 10‰ to warrant a split of zones. For this reason the unsaturated zone of water availability for plants was assigned as one zone. From this the transpiration has been partitioned into saturated and unsaturated zone transpirations.

3.2.5. Spatial upscaling of T_g

The fundamental element in transpiration upscaling is the assessment of individual tree transpiration and species dependent upscalling functions (Mapanda, 2003). Following the isotopic partitioning of transpiration into the Tg and Tu, for each species, Tg was mapped into the catchment using BUF and f_g derived per species. The BUF was used to derive the sapwood area from the canopy area retrieved through RS and GIS application over the QuickBird® image, while f_g to define species dependent contributions of Tg in the total tree transpiration.

4. Results and Discussion

Plants take water from unsaturated or saturated zones depending on the hydrological setting and the adaptation mechanisms of the species present in the catchment (Lubczynski, 2009). Direct tree root tapping from aquifer system influences the groundwater balances (Snyder and Williams, 2000). Knowing where the plants source water used for transpiration, opens the way to understand better the not only tree physiology but also its hydrological importance.

4.1. Sap flow Analysis

HFD Sensor Sap flow

The TDP method measure sap flux density (SFD) at two centimeters only. Various investigations showed that the SFD varies with sapwood depth (Köstner et al., 1998; Lu et al., 2004; Tateishi et al., 2008; Wullschleger and King, 2000). The results from HFD show the variation in the SFD with depth, in accordance with studies of (Čermák et al., 2004; Nadezhdina et al., 2004; Wullschleger and King, 2000). In the study of Wullschleger and King (2000) they hypothesized that "*the fraction of sapwood functional in water transport would decrease as either stem diameter or sapwood thickness increased*". The highest sap flux densities are usually in the outer sapwood contributing most to the whole tree sap flow. As depth increases, sap flux density usually decreases towards the heartwood. However, the variation in SFD with depth is not linear (Wullschleger and King, 2000).

The DBH measured in the field for *Q.i.* analysed in this study was 28.0cm and sapwood depth 6.5 cm. In *Q.i.* the variation of sap flux density with sapwood radial depth showed a pattern different from the above hypothesis. The high flux density was rather towards the inner sapwood. This was evident in mean sap flux density taken at the peak SFD period (12h – 16h). In Figure 12 (a, c) the pattern for the 1 day mean and that of 12day mean are almost equal. The most active part of the sapwood in *Q.i.* is the 5.5cm and 6.5cm as much of the flux density is routed through this zone. There is no direct relationship between the sap flux density and sapwood depth, disagreeing with Wullschleger and King's (2000) statements.

The *Q.p.* analyzed in this study had 43.0 cm DBH and sapwood depth of 5.3 cm. The radial sap flux density pattern was different than that of *Q.i.* It followed the hypothesis of Wullschleger and King (2000) i.e. much of the sap flux density was concentrated in the outer sapwood and decreased towards heartwood. The majority of sap flow was concentrated within the first 0 – 3.5 cm (Fig.12). The relation of SFD with depth was not linear and could well be fitted with an exponential function as indicated by Köstner (1998) or a log function (See Figure 12 c & d) with (R^2 = 0.9). The obtained results indicated the radial variation of SFD with sapwood depth might be species dependent. The sap flux density - sapwood radial variation pattern shown by both species diverge clearly from each other as shown in Figure 12. In my opinion, this divergence might be attributed to the anatomical structure of the sapwood for each species.

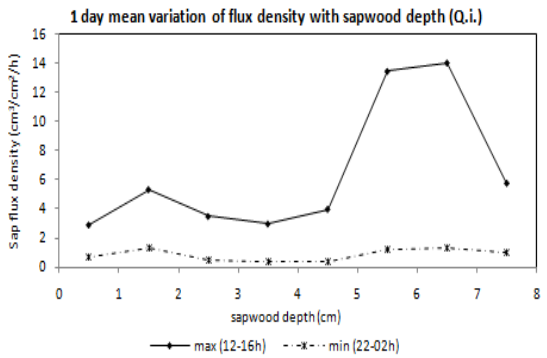

a) Mean 1 day sap flux density variation with sapwood depth in *Q.i.*

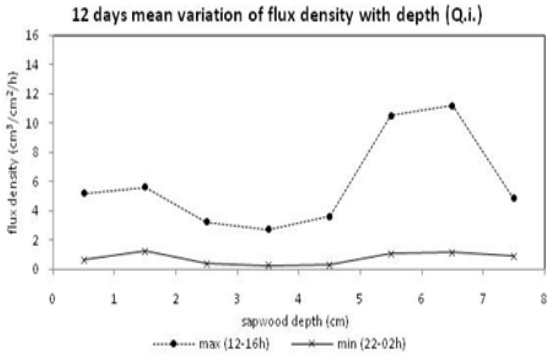

b) Mean 12 days sap flux density variation with sapwood depth in *Q.i.*

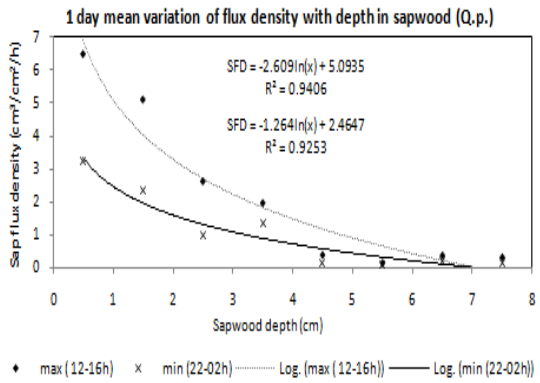

c) Mean 1 day sap flux density variation with sapwood depth in *Q.p.*

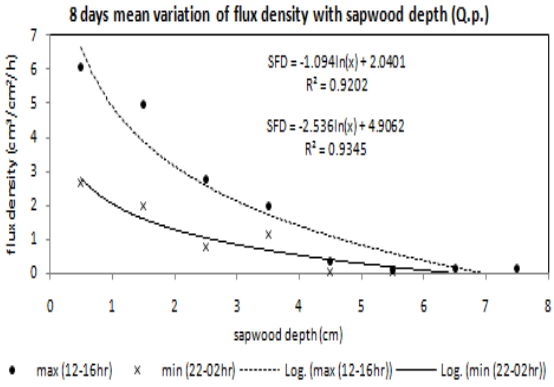

d) Mean 12 days sap flux density variation with sapwood depth in *Q.p.*

Figure 12: Radial variation of sap flux

Figure 13 and 14 showed the 3d view of the variation of SFD within the various sensing depths. The 6.5 cm and 0.5 cm depths turned to be critical while comparing SFD of the selected *Q.i.* and *Q.p.*

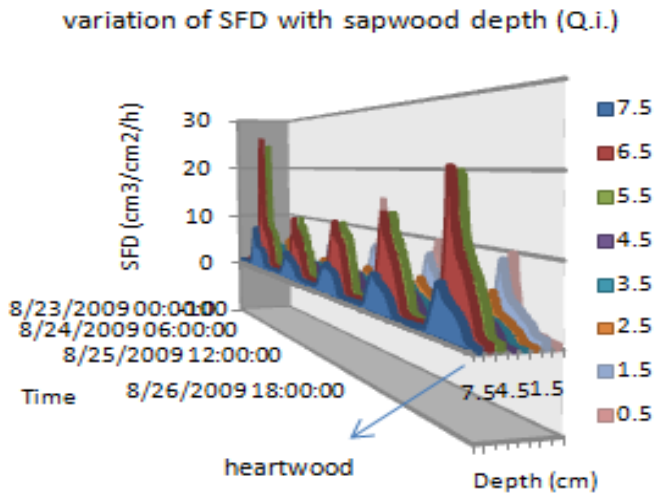

Figure 13: Variation of sap flux density with sapwood depth in (*Q.i.*)

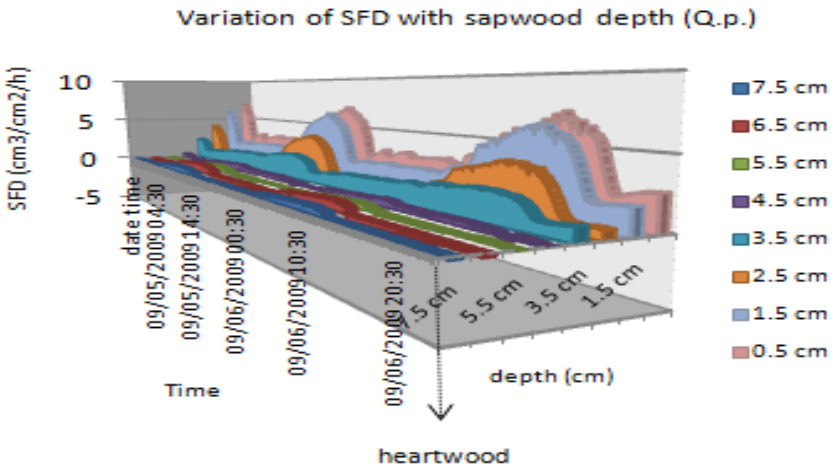

Figure 14: Variation of sap flux density with sapwood depth in *Q.p.*

TDP Sensor Sap flow

The TDP sensors connected to a CR 1000 Campbell Logger, were installed to check circumferential and axial sap flux density variations in the stem. Figure 15 shows the circumferential and axial variations in sap flux density in a *Q.i.* The sensor connected close to the ground showed the highest peak sap flux density 31 $cm^3/cm^2/h$ on day 209 10:00 am whilst the one connected to the first branch level the lowest peak flux density is $9cm^3/cm^2/h$ day 206 at 2:00 pm. The diurnal variation of sap flux density follows the same pattern in all direction increasing sharply in the morning and reaching the peak at the midday.

It could be assumed that high peak sap flux density recorded by the sensor close to the ground is as a result of ambient temperature around the ground level. The sap flux density decreases towards the crown. The east facing sensor at 1.3m (breast height) also recorded highest among the directions of east west, south and north. The main cause of circumferential variation is direct exposure to sun ray (Lu et al., 2000). Circumferential variation is influenced by tree separation (Lu et al., 2000).

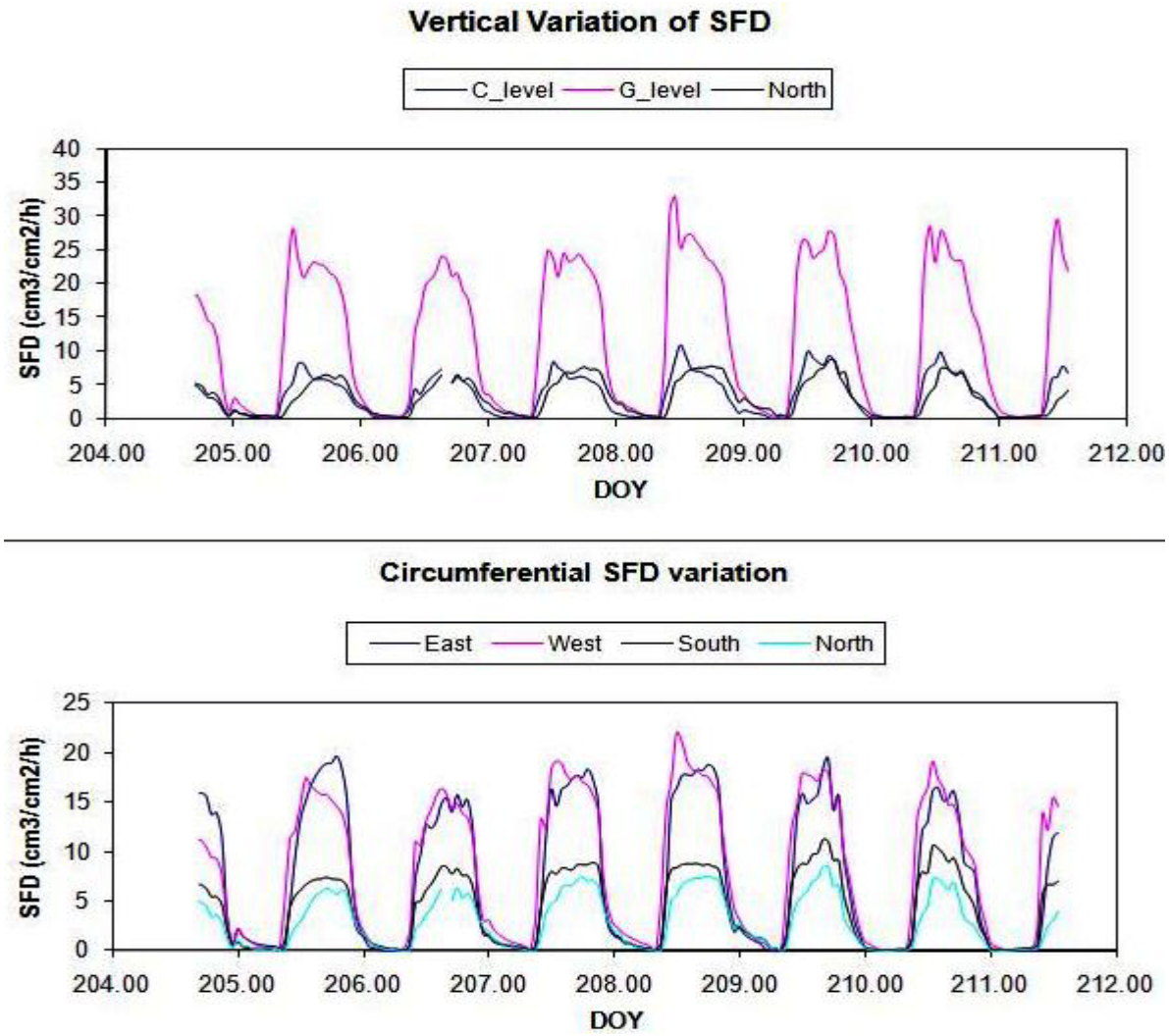

Figure 15: Axial and circumferential variation of sap flux density of *Q.i.* as measured by TDP

The average sap flux density for *Q.i.* of the six sensors for Julian day 205 to Julian day 211 of June 2009 is as shown in Figure 16. This resulted in a maximum peak of 15.3cm^3/cm^2/day at midday and the minimum was zero within this period.

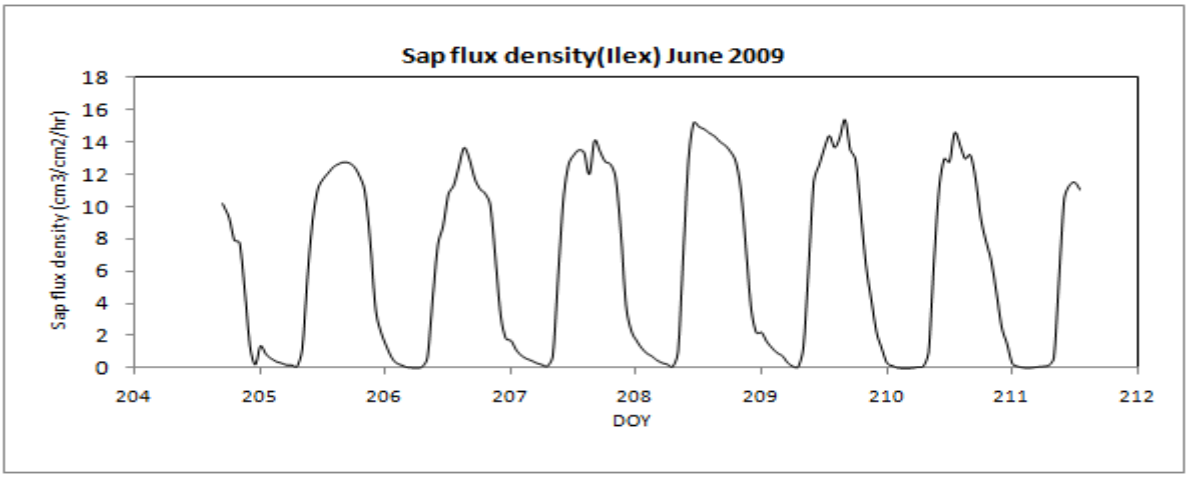

Figure 16: Integrated 30 min – hourly sap flux density for *Q.i.* in June 2009 as measured by TDP

In Figure 17, the average hourly sap flux density for the months of June, July, August and September is presented with the month of August showing a higher peak of 13.8 cm3/cm2/h for *Q.i.* and 12.5cm3/cm2/h for *Q.p.* The flow of sap flux delays in the months of September as it starts flowing after 8:00 hours whilst in June it start flowing as early as before 7:00 hours in *Q.i.* This might be attributed to variation in sunrise hours as photosynthesis is driven by sunlight. It could be observed that there is a difference in response to morning and evening sunray by both species. As *Q.p.* reaches its peak as a response to the morning and evening sunray and flattens between 10:00 – 20:00h *Q.i.* reaches its peak around midday between 10:00 – 20:00h. Another difference is that evergreen *Q.i.* SFD has approximately the same rate through the dry season while deciduous *Q.p.* declines its SFD which is likely related to the decline of its photosynthetic activities.

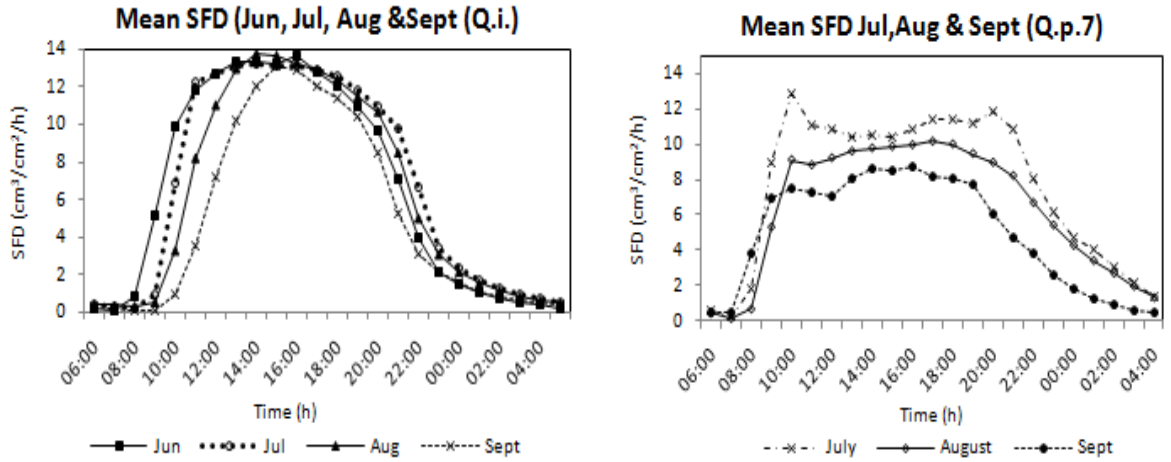

Figure 17 : Mean diurnal sap flux density for Q.i. & Q.p. in dry season 2009 as measured by TDP

In Figure 18(a) the Q.p. have different diameters. The diameters are 17.5cm, 22.28cm and 28.65cm for *Q.p.* 2, 3, and 1 respectively and consequently the sap flux density also follows with the higher peak recorded by the larger DBH *Q.p* 1. Eventually, the comparing Figure 18a and b which also show the same trend as the *Q.p.* in (a) have smaller diameter as compared with the one in (b) DBH of 38.20cm with the sap flux density in (b) higher than that of (a).

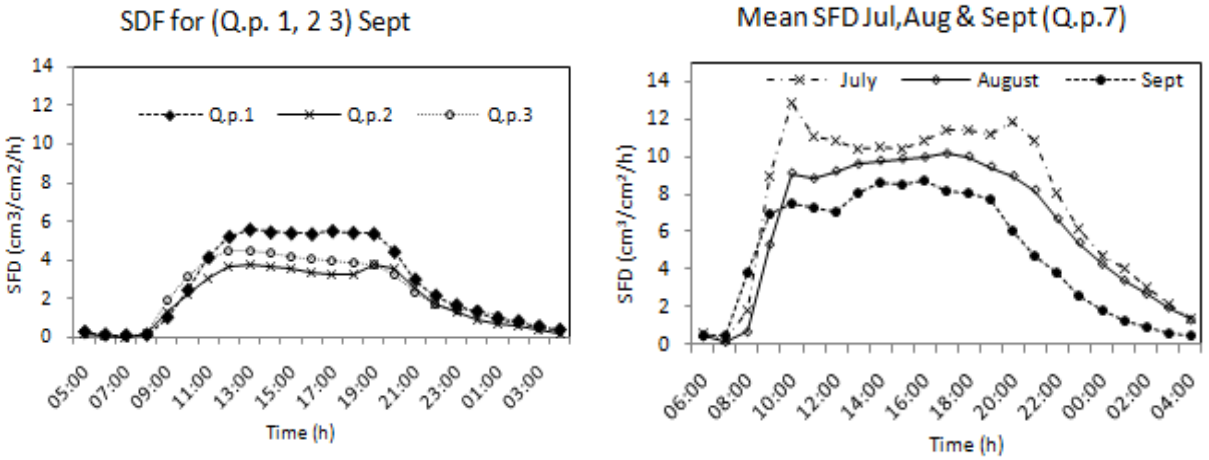

a)TDP sap flux density of *Q.p* 1,2&3 in Sept.

b) TDP Sap flux density of *Q.p.* 7

Figure 18: Integrated TDP sap flux density for different DBH of *Q.p.*

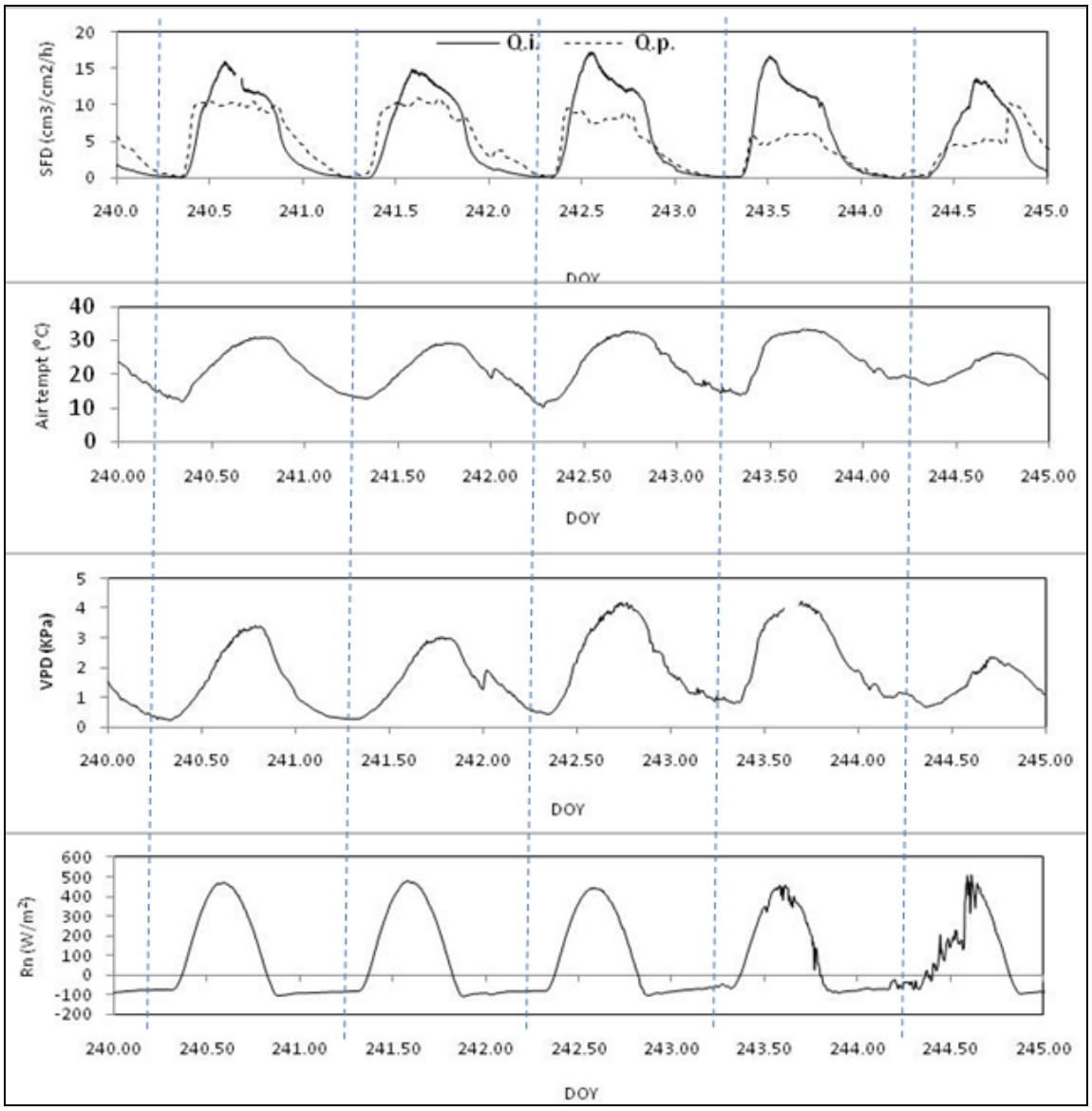

Figure 19: Variation of SFD, air temperature, vapour pressure deficit and net Radiation for Q.i., Q.p. 27Aug – 01 Sept (Net radiation, air temp, vapour pressure deficit, processed by Rwasoka (2010))

Figure 19 shows the SFD for *Q.i.* and *Q.p*, the air temperature, vapour pressure deficit VDP, and net radiation Rn for *Q.i.* and *Q.p* from 27 August to 01 September. The maximum air temperature for the period was 33°C and the minimum of 9.03°C and the mean value of 21°C. In case of the VPD, the maximum is 4.22kPa, minimum of 0.17kPa with a mean of 1.62kPa as in Figure 20. Within the same period, the maximum and minimum net radiations are 566.33W/m2 and -116.81W/m2 and the mean value of 82.72W/m2. The sap flux density of deciduous *Q.p* seemed to be responsive to the VPD within the period. As the VPD increases, the SFD also increases.

Canopy Transpiration (Tc)

Scaling from stem to tree level was done by normalizing the mean transpiration computed for each species over the study period with the mean crown area according to equation 6. This resulted in a peak value of 3.19 mm/day and 1.66mm/day and mean value of 1.47mm/day and 1.03mm/day for Q.i. and Q.p. as shown in Figure 20.

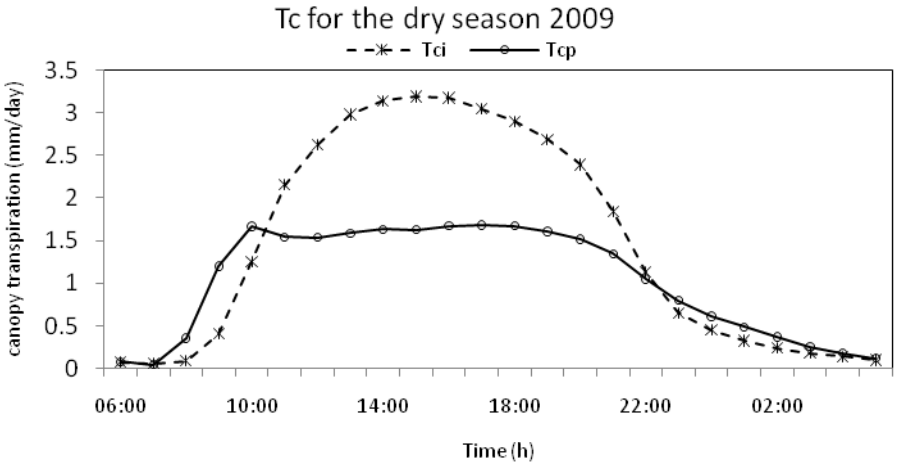

Figure 20: Canopy transpiration for Q.i. and Q.p. for the dry season 2009

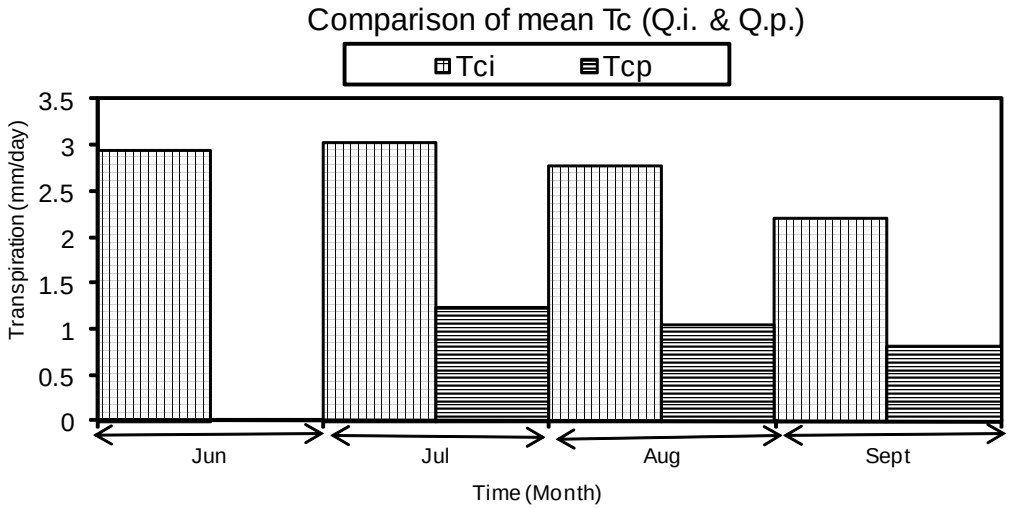

Figure 21: Monthly variation of tree transpiration

From Figure 21 & 22, the transpiration reduces from month to month as the dry season progresses. As the sun radiation and soil water content decreases while vapour pressure deficit increases, from June to September, the transpiration rate also decreases. In the study of Lu et al. (2000) he fund that the sap flux density decreased about 35% from wet to dried condition.

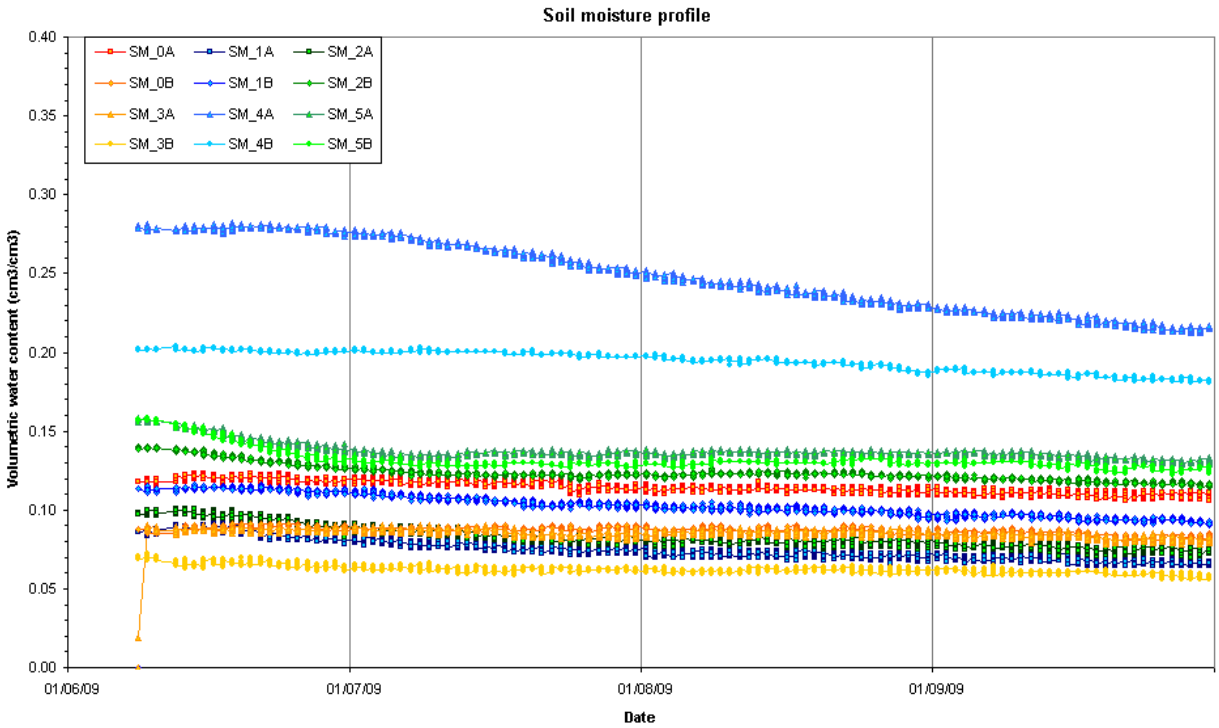

Figure 22: Variation of soil moisture content (processed by Alain Pascal, unpublished)

Biometric Characteristics

The inventory of the biometric data indicated bigger stem size among *Q.i.* than *Q.p.* The analysis of database of 24 *Q.i.* and 21 *Q.p.* indicated minimum and maximum diameter at breast height (DBH) from 0.16m to 0.8m for *Q.i.*, and from 0.18m to 1.05m *Q.p.* respectively. The mean values are 0.45m and 0.46m with standard deviations of 0.21m and 0.30m for *Q.i.* and *Q.p.* (see Table 2 and Table 3). *Q.i.* showed high values in case of sapwood depth. The minimum sapwood depth measured for *Q.i.* was 0.03m and the maximum is 0.07m with a mean value of 0.05m. In the case of Q.*p.* sapwood depth ranged between 0.02m and 0.06m, with a mean value of 0.03m. The *Q.i.* canopy areas were between 20.31m^2 and 124.69m^2 with a mean of 58.83m^2 the *Q.p.* between 15.14m^2 and 191.13m^2, with 62.54m^2 mean.

	DBH (m)	x (m)	Cc (m)	As (m^2)	HB (m)	Ax (m^2)	Ac (m^2)
max	0.80	0.07	12.60	0.50	2.600	0.125	124.69
min	0.16	0.03	5.09	0.02	1.100	0.015	20.31
median	0.35	0.05	8.00	0.10	1.840	0.046	50.27
1st Qu	0.29	0.04	6.46	0.07	1.665	0.034	32.80
3rd Qu	0.67	0.06	9.93	0.36	2.000	0.078	77.50
mean	0.45	0.05	8.35	0.19	1.853	0.057	58.83
stdev	0.21	0.01	2.31	0.16	0.327	0.030	32.56

Table 1: Summary Statistics of *Q.i.* Biometric Data

DBH: diameter at breast height, x: xylem depth, HB: height at first branch, Ax: sapwood area, Ac: canopy area and As: stem area, Cc: canopy diameter

	DBH (m)	x (m)	Cc (m)	As (m^2)	HB (m)	Ax (m^2)	Ac (m^2)
max	1.05	0.06	15.60	0.87	2.600	0.137	191.13
min	0.18	0.02	4.39	0.03	1.600	0.009	15.14
median	0.33	0.04	7.19	0.08	2.050	0.029	40.60
1st Qu	0.23	0.03	5.70	0.04	1.870	0.016	25.52
3rd Qu	0.66	0.04	10.90	0.34	2.400	0.066	93.31
mean	0.46	0.03	8.37	0.23	2.080	0.045	62.54
stdev	0.297	0.009	3.157	0.273	0.292	0.037	47.462

Table 2: Summary Statistics of *Q.p.* Biometric Data

In order to upscale the transpiration to the catchment level, a remote sensing approach was used to retrieve the canopy areas for each species using a multispectral image (Quickbird®). This was used to retrieve the sapwood area through their correlation with canopy areas using the BUF for the spatial representation of the transpiration.

4.2. Upscaling of transpiration

Biometric Upscaling Functions (BUF)

For spatial representation of the transpiration it is important to determine scalars which can be retrieved from remote sensing (Chavarro-Rincón, 2009). The establishment of biometric upscaling functions (BUF) to relate the variability of scalars to the sap flow in order to upscale them to the catchment level, is very important in a transpiration study. The biometric data was correlated to a scalar (A_x) using linear regression analyses. Among them, DBH – sapwood area, canopy area – DBH and canopy area – sapwood area provides strongest correlation as in Figure 24. This was done using 24 trees for Q. i. and 21 trees for Q.p. Table 3 & 4

	DBH (m)	x (m)	Cc (m)	As	HB (m)	Ax (m2)	Ac (m2)
1	0.80	0.04	11.50	0.50	2.00	0.097	103.869
2	0.73	0.04	10.20	0.42	2.00	0.077	81.713
3	0.16	0.06	5.50	0.02	1.40	0.015	23.758
4	0.78	0.04	12.50	0.47	1.80	0.099	122.718
5	0.67	0.03	8.70	0.35	2.10	0.063	59.447
6	0.26	0.07	6.10	0.05	1.10	0.037	29.225
7	0.35	0.06	8.00	0.10	1.80	0.051	50.265
8	0.32	0.05	8.60	0.08	1.75	0.042	58.088
9	0.35	0.05	7.80	0.10	1.60	0.043	47.784
10	0.37	0.05	7.00	0.11	1.50	0.048	38.485
11	0.28	0.03	5.60	0.06	1.65	0.024	24.630
12	0.29	0.04	6.40	0.07	1.75	0.030	32.170
13	0.29	0.04	6.50	0.07	1.60	0.029	33.183
14	0.30	0.04	6.70	0.07	2.10	0.031	35.257
15	0.59	0.07		0.27	2.55	0.107	
16	0.31	0.06	8.00	0.08	1.90	0.044	50.265
17	0.32	0.04	7.50	0.08	1.88	0.035	44.179
18	0.22	0.06	5.09	0.04	1.72	0.027	20.308
19	0.46	0.05	9.66	0.17	1.96	0.065	73.290
20	0.69	0.04	12.13	0.37	2.60	0.079	115.466
21	0.72	0.06	12.60	0.40	2.10	0.125	124.690
22	0.28	0.06	6.43	0.06	1.67	0.038	32.422
23	0.75	0.04	10.20	0.45	2.00	0.092	81.713
24	0.47	0.06	9.45	0.17	1.94	0.071	70.138

DBH: diameter at breast height, x: xylem depth, HB: height at first branch, Ax: sapwood area, Ac: canopy area and As: stem area, Cc: canopy diameter

Table 3: Biometric characteristics of *Q.i.*

	DBH (m)	x (m)	Cc (m)	As (m2)	HB (m)	Ax (m2)	Ac (m2)
1	1.05	0.03	13.4	0.867	2.1	0.104	141.026
2	0.93	0.04	10.4	0.679	2.1	0.095	84.949
3	0.75	0.04	10.9	0.443	2.05	0.084	93.313
4	1.02	0.05	15.6	0.815	1.8	0.137	191.134
5	0.35	0.06	7.5	0.096	2.5	0.047	44.179
6	0.31	0.02	6.6	0.075	1.8	0.019	34.212
7	0.22	0.03	5.2	0.039	1.8	0.016	21.237
8	0.76	0.04	12.3	0.458	2	0.078	118.823
9	0.20	0.02	4.9	0.032	1.9	0.011	18.857
10	0.23	0.03	5.6	0.042	1.6	0.018	24.630
11	0.23	0.02	5.5	0.043	2.5	0.012	23.758
12	0.23	0.03	6.625	0.042	1.88	0.017	34.472
13	0.66	0.03	9.45	0.344	2.6	0.058	70.138
14	0.24	0.04	6.7	0.044	2.4	0.021	35.257
15	0.33	0.05	6.88	0.083	2.4	0.035	37.176
16	0.20	0.02	4.39	0.031	1.7	0.009	15.136
17	0.21	0.04	7.19	0.035	1.93	0.016	40.602
18	0.62	0.04	11.43	0.303	2.4	0.063	102.608
19	0.18	0.04	5.7	0.025	1.87	0.015	25.518
20	0.66	0.04	11.65	0.342	2.2	0.066	106.596
21	0.34	0.03	7.95	0.092	2.15	0.029	49.639

DBH: diameter at breast height, x: xylem depth, HB: height at first branch, Ax: sapwood area, Ac: canopy area and As: stem area, Cc: canopy diameter

Table 4: Biometric characteristics of *Q.p.*

The relationship between canopy – sapwood areas showed a strong correlation with about 0.90 coefficient of determination in *Q.p.* and 0.91 coefficient of determination in *Q.i.* as shown in Figure 23. The Pearson correlation was 0.9538 and 0.9475 for *Q.i.* and *Q.p.* respectively.

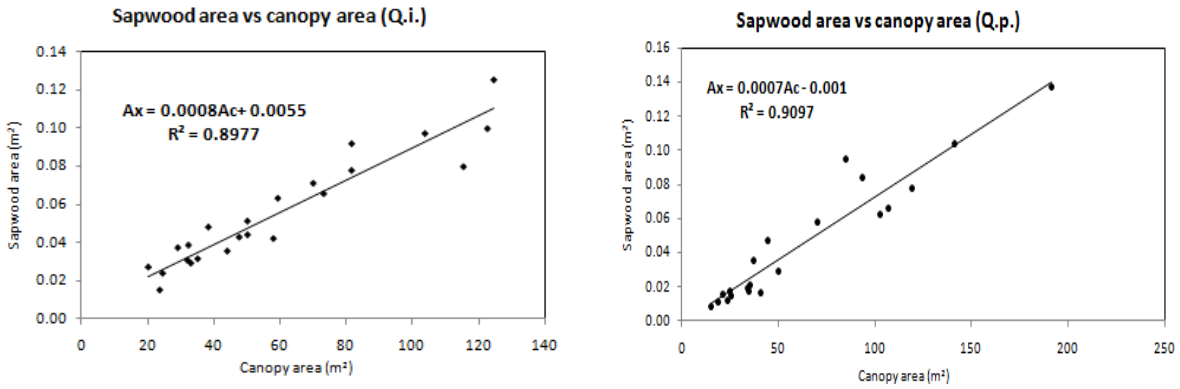

Figure 23: Biometric upscaling function for Q.i. and Q.p.

Spatial representation of transpiration

In other to move from the individual tree level to the catchment level, biometric upscaling functions were developed as in (relation 14 & 15). The spatial representation of the transpiration on catchment was based on canopy areas retrievals. This uses the application of remote sensing, RS based vegetation classification and canopy delineation (Chavarro-Rincón, 2009). The upscaling was done based on retrieved canopy area from remote sensing image of Quickbird. In this, A_c was applied the upscaled scalar though considered as less accurate but efficient (Lubczynski, 2009). The canopy area was obtained from a vegetation classification of Salinas (2010) and application of BUF to upscaled the v, hence the sap flow (14 & 15).

The following Equations 10 and 12 were derived from Equation 1 and the Equations 11 and 13 from Equation 6

$$Q_i = (0.0008A_{ci} + 0.0055)v_i \quad \textbf{7}$$

$$T_{ci} = \frac{(0.0008A_{ci} + (0.0055))v_i}{A} \quad \textbf{8}$$

$$Q_p = (0.0007A_{cp} - 0.0010)v_p \quad \textbf{9}$$

$$T_{cp} = \frac{(0.0007A_{cp} - 0.0010)v_i}{A} \quad \textbf{10}$$

where A_{ci} and A_{cp} are canopy areas retrieved from the images [L^2]; v_i and v_p sap flux densities for Q.i. and *Q.p.* [L/T]. Q_i and Q_p are sap flow [L3/T] for *Q.i.* and *Q.p.* and T_{ci} and T_{cp} are canopy transpirations of *Q.i.* and *Q.p.* in [L/T]

The mean dry season canopy transpiration over the La Mata catchment for *Q.i.* is 0.61 mm/day and for *Q.p* is 0.72 mm/day. The local variability of tree transpiration can be analyzed within the selected in the La Mata catchment stand (plot) of 1 ha (Fig.1). The variability of canopy tree transpiration in the selected stand can be observed in Figure 24. In the dry season 2009, the canopy transpiration in the selected plot ranges were 0.020 – 0.734 mm/day and 0.035 – 0.927 mm/day for *Q.i.* and *Q.p* respectively with mean values of 0.022 mm/day and 0.0037 mm/day for *Q.i.* and *Q.p.* respectively. These values are higher than the September values which range 0.013 – 0.415 mm/day and 0.0200 – 0.645 mm/day with mean values of 0.018 mm/day and 0.039mm/day for *Q.i.* and *Q.p.* In Figure 24 (e and f) the total canopy tree transpiration distribution is shown with value range of 0.022-0.615 mm/day and 0.018-0.645 mm/day in the dry season 2009 and September 2009.

The plot and catchment transpiration results are influenced by canopy clustering. Areas with dense canopy coverage show higher transpiration as in individual tree transpiration per area is higher than that of isolated canopies. Further, it could be observed that the distribution of the transpiration does not only vary temporally, but it is influenced by the species composition of trees and size of the canopies. The accuracy of this solution is dependent on the species classification, accuracy of the BUF used and the accuracy of the retrieval of the canopy areas (Lubczynski, 2009).

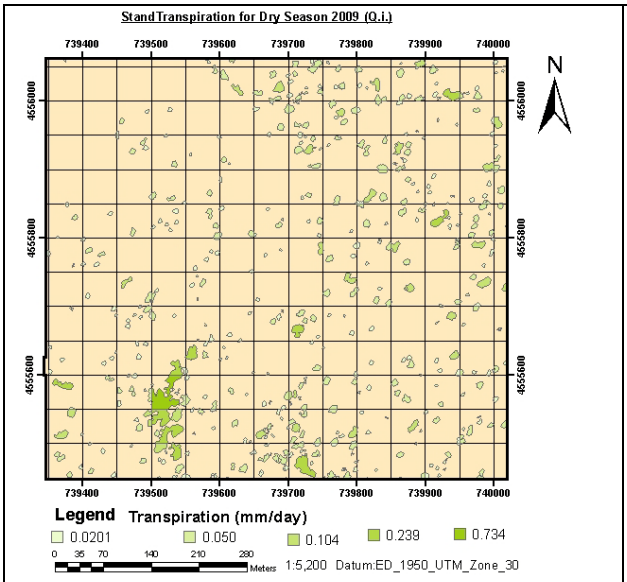

a) Plot canopy transpiration for Q.i. in dry season 2009

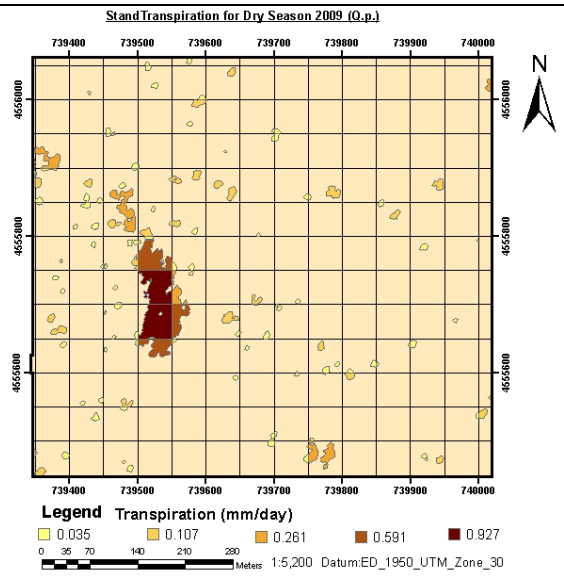

e) Plot canopy transpiration for Q.p. in dry season 2009

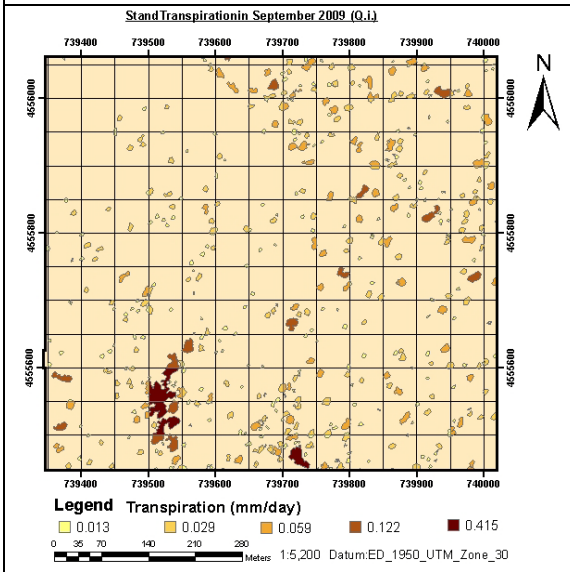

c) Plot canopy transpiration for Q.i in September 2009

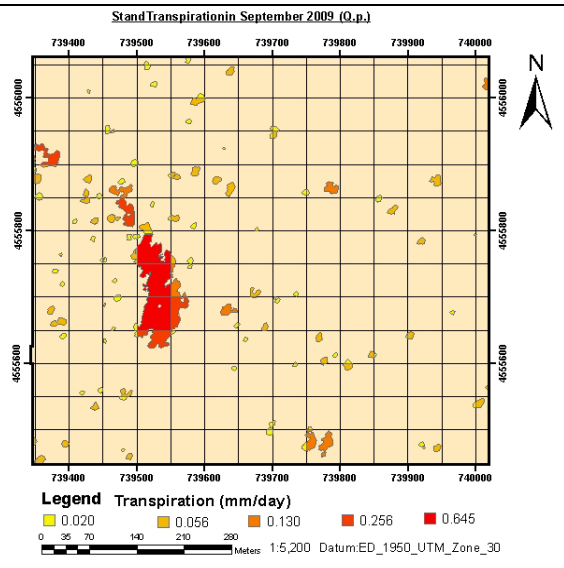

d) Plot canopy transpiration for Q.p. in September 2009

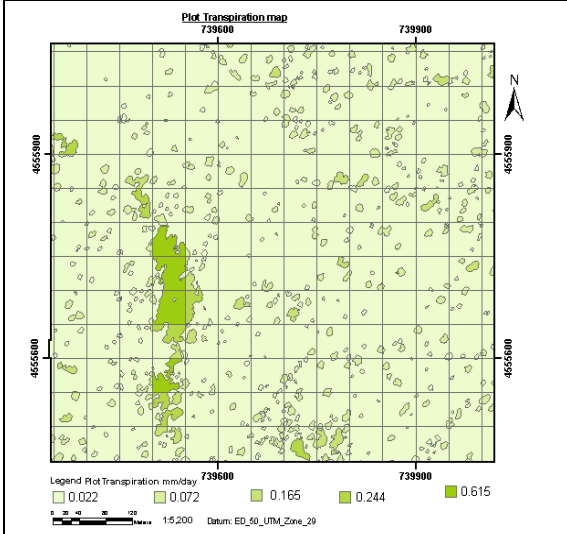

e) Plot canopy transpiration for the dry season 2009

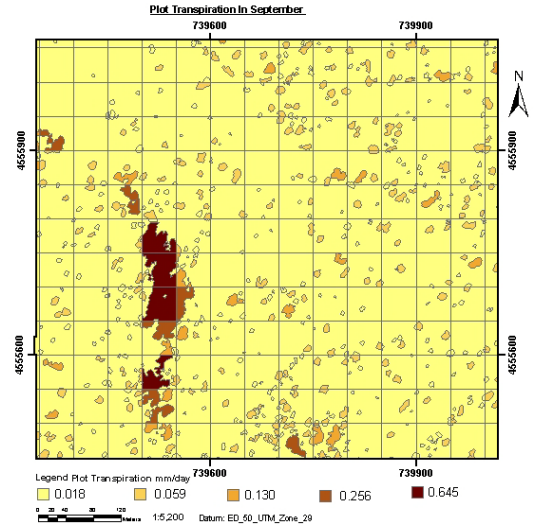

f) Plot canopy transpiration for September 2009

Figure 24: Mean canopy transpiration distribution in the catchment

The plot transpiration

Using a plot size of 1 ha the distribution of the transpiration is as shown in Figure 25 transpiration varies from 0.016 to 0.517 mm/d with a mean value of 0.061 mm/day. The distribution of the transpiration varies depending on the species type of tree and the density of the canopy.

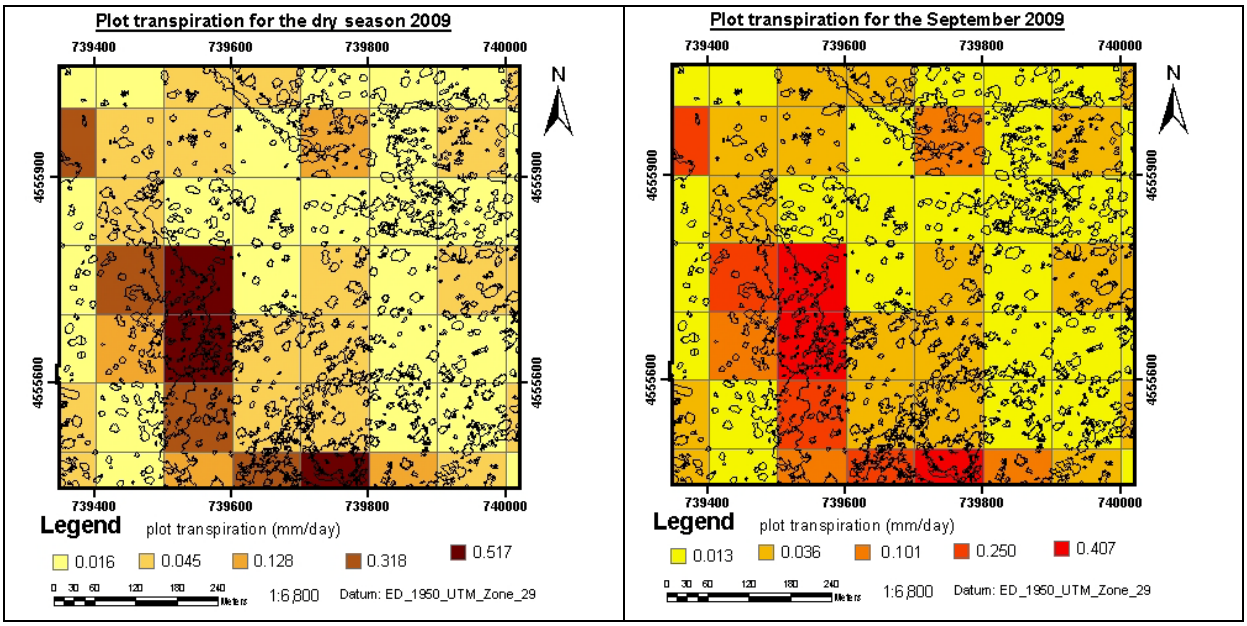

Figure 25 : Spatial representation of plot transpiration

4.3. Soil Matric Potential

At the isotope tracing sites where the samples for matric potential assessment were taken, the water table was shallow 1.10 m b.g.s. Generally, wilting point is assumed to be at -1.5 MPa (Dingman, 2002). At the point close to the ADAS station (bare soil in Figure 25), the minimum matric potential recorded was -3.5 MPa at 25 cm depth and the maximum -0.2 MPa at 100cm depth. Under *Q.p.* (Figure 26 a & b), the minimum matric potential was -4.38 MPa at the northern side and -11.8MPa at a depth of 25cm in the southern side. The maximum values are -0.017MPa and 0.09MPa at the depth of 100cm in the southern direction. Around the *Q.i.* (Figure 26 c & d), minimum values are -2.05MPa and -5.62MPa at a depth of 25 cm in the northern and southern direction respectively whilst the maximum values are -0.19 3MPa and -0.527 MPa at the depth of 75cm in the northern and southern direction respectively.

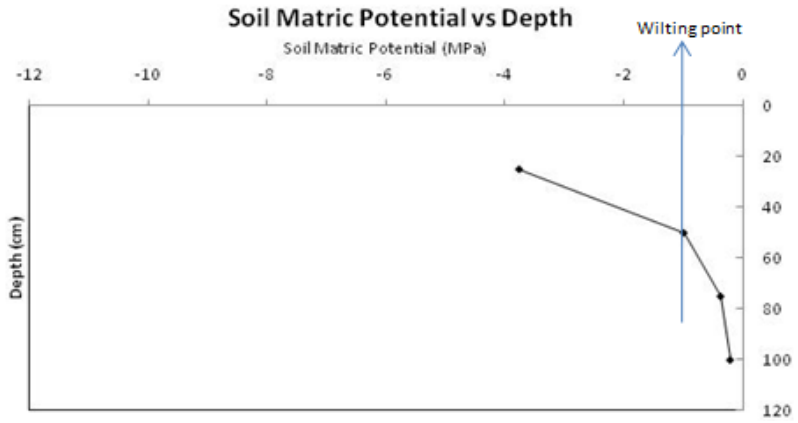

Figure 26: Soil matric potential profile for bare area

The results indicates that the soil was very dry in the top layer so it is assumed that there was no water available for the trees in the depth of (0-60cm) as the water potential reached or was very close to the wilting point (Figure 26). Thus trees are probably sourcing water from deeper levels. In the case of *Q.i.,* varies studies show its phreatophytic behaviour (Corcuera et al., 2004; David et al., 2007; Lubczynski and Gurwin, 2005), indeed suggesting *Q.i.* water uptake from below 60cm. In the case of *Q.p.* it has been reported by previous studies that this species has dense root system to a depth of 60cm and a single tap root (Hernández-Santana et al., 2008; Silva et al., 2003; Silva and Rego, 2004). With this in mind, the section from which the water is taken can be divided into two. That are saturated and unsaturated zones.

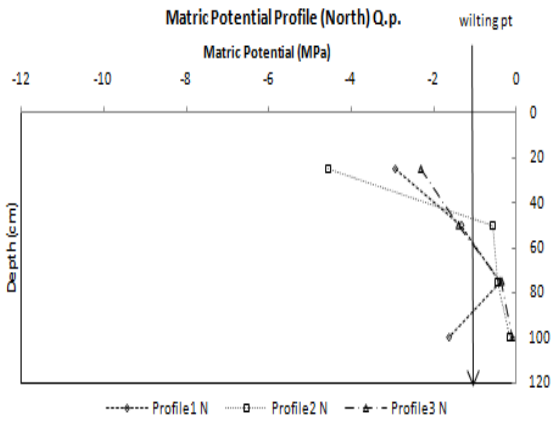

a) Matric potential under Q.p. (North direction)

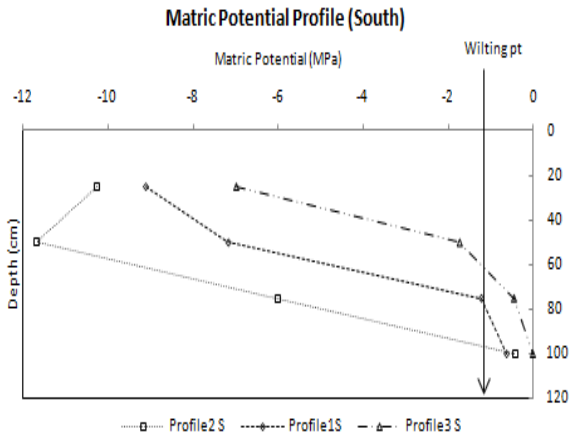

Matric potential under Q.p. (South direction)

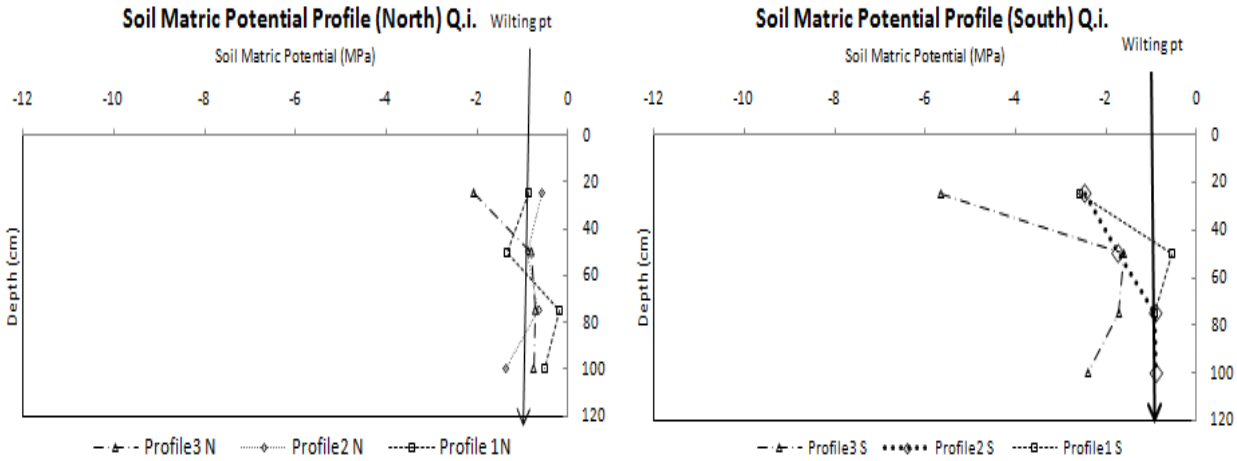

c Matric potential under Q.i. (North direction) d Matric potential under Q.i. (South direction)

N: north, S: south

Figure 27: Soil Matric potential profile under Q.i. and Q.p.

4.4. Isotope tracing

An end member approach relating the deuterium composition in the soil, groundwater and the xylem-sap, was used in the analysis of the water sources partitioning of the plant. The data collected from these sources was complemented with measurements of soil matric potential, which helps in limiting the zones from which plants take water when formulating the mixing model. The possible depth and the deuterium composition under each tree species is shown in Table 5.

The result of the soil deuterium profile did follow the general theory of the heavier isotopes at the top graduating downwards (Figure 27) in both cases of profile taken. In the case of both *Q.i.* and *Q.p.*, there is a gradual decrease in heavier isotopes from 25-100cm.

Date	δ^2H (‰) Q.p.	δ^2H (‰) Q.i.	depth (cm)
10/09/2009	-33.40	-23.54	25.0
10/09/2009	-35.08	-32.89	50.0
10/09/2009	-41.23	-34.70	75.0
10/09/2009	-45.83	-38.07	100.0
	-40.71	-35.22	

δ^2H(‰)Q.p.: deuterium ratio in soil under Q.p. δ^2H(‰)Q.i.: deuterium ratio in soil under Q.i.

Table 5: Table of soil deuterium values for Q.i. & Q.p.

As indicated from section 4.3, the zones (0-50cm) in case of Q.i. and (0-60cm) for Q.p. have low matric potential and are not a good water uptake sources. In addition, the difference in the δ^2H values for the unsaturated zone with availability of water for plants (in Figure 27) is not more than 10‰. Based on these, two compartment models were designed for the analysis taking the whole unsaturated zone as one compartment and the saturated zone as another compartment.

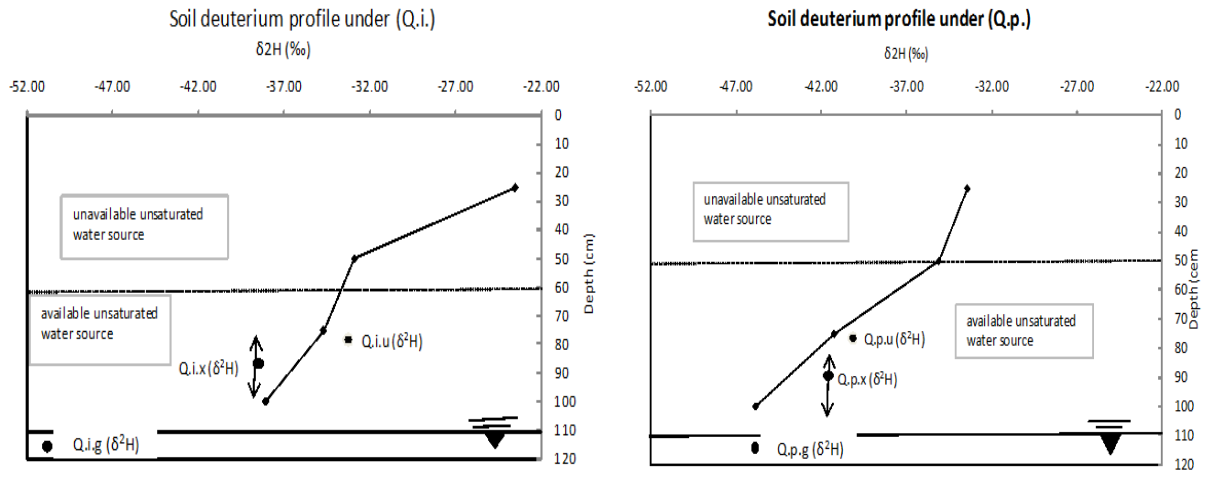

Figure 28: Soil deuterium profile under both *Q.i.* and *Q.p.*

Two compartment source mixing model of saturated and unsaturated zone water sources have been used in this analysis (David et al., 2007). The result from the various zones is as plotted in Figure 28 which shows the variation of the δ^2H composition over the period. The variation pattern of deuterium isotopes in the sap-water follows similar pattern as that of the groundwater. That means there is a relation between the deuterium composition in the groundwater and the sap-water.

In the estimations the deuterium composition in the soil was assumed to be constant over the period of monitoring as shown in Figure 28. The mixing model analysis result is as shown in Table 6 for *Q.i.* and Table 7 for *Q.p.*

In each case the mean value of the fractional contribution over the monitoring period calculated.

Deuterium composition (Q.i.)					
Date	d2H (‰) Gw	d2H (‰) Sw	(dH-2 [‰] Uw	fg	fu
22/08/2009	-51.9726				
22/08/2009	-50.4914				
23/08/2009	-49.9309	-44.6611	-35.2195	0.36	0.64
23/08/2009	-50.4997	-39.8461	-35.2195	0.70	0.30
23/08/2009	-50.0703	-40.2755	-35.2195	0.66	0.34
23/08/2009	-51.6645	-41.2509	-35.2195	0.63	0.37
23/08/2009	-51.3247				
24/08/2009	-51.1658				
24/08/2009	-51.3487				
24/08/2009	-51.9328	-43.6396	-35.2195	0.50	0.50
24/08/2009	-50.3946	-41.7761	-35.2195	0.57	0.43
25/08/2009	-50.8543	-39.7389	-35.2195	0.71	0.29
26/08/2009	-49.3047	-39.9623	-35.2195	0.66	0.34
27/08/2009	-50.3885	-37.6386	-35.2195	0.84	0.16
28/08/2009	-48.0660	-35.9657	-35.2195	0.94	0.06
29/08/2009	-49.6367	-39.6219	-35.2195	0.69	0.31
20/09/2009	-48.3469	-35.1257	-35.2195		
			Mean	0.69	0.31

δ^2H(‰)Gw : deuterium ratio in groundwater, δ^2H(‰)Uw: deuterium ratio in unsaturated zone δ^2H(‰)Sw : deuterium ratio in xylem

Table 6: Fractional components of the two sources for (*Q.i.*)

Deuterium composition (Q.p.)					
Date	d2H (‰) Gw	d2H (‰) Sw	(dH-2 [‰] Uw	fg	fu
05/09/2009	-46.9227				
05/09/2009	-47.9571				
05/09/2009	-48.0017	-43.7829	-40.7133	0.58	0.42
06/09/2009	-46.5828	-40.6098	-40.7133		
06/09/2009	-46.8573	-42.1317	-40.7133	0.77	0.23
06/09/2009	-46.8603	-42.2819	-40.7133	0.74	0.26
06/09/2009	-46.6953	-42.7556	-40.7133	0.66	0.34
06/09/2009	-45.6451	-41.6855	-40.7133	0.80	0.20
07/09/2009	-46.8247	-42.0605	-40.7133	0.78	0.22
07/09/2009	-47.2839	-42.4507	-40.7133	0.74	0.26
07/09/2009	-46.3489				
07/09/2009	-45.6263				
08/09/2009	-46.8335				
09/09/2009	-45.6100	-40.3356	-40.7133		
10/09/2009	-47.5320	-41.5208	-40.7133	0.88	0.12
11/09/2009	-47.4809	-43.6147	-40.7133	0.57	0.43
12/09/2009	-45.3731	-42.8850	-40.7133	0.53	0.47
20/09/2009	-45.5594	-42.1989	-40.7133	0.69	0.31
			Mean	0.76	0.24

δ^2H(‰)Gw : deuterium ratio in groundwater, δ^2H(‰)Uw: deuterium ratio in unsaturated zone δ^2H(‰)Sw : deuterium ratio in xylem

Table 7: Fractional component of the two sources (*Q.p.*)

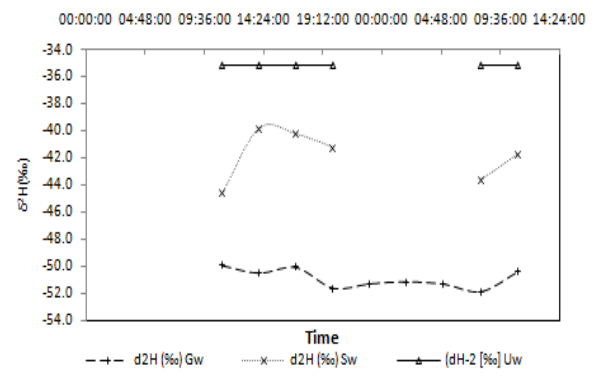

(a) 24hr groundwater and sap water deuterium composition monitoring under Q.i.

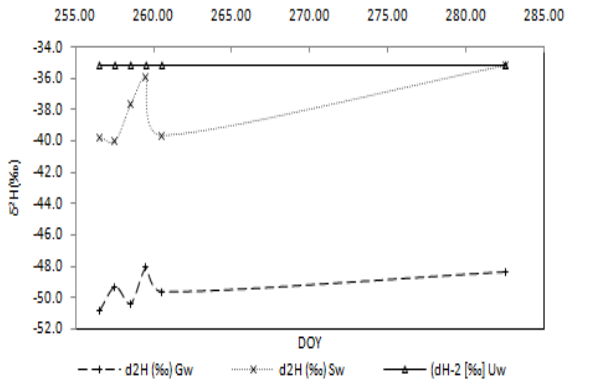

(b) daily groundwater and sapwater deuterium monitoring under Q.i.

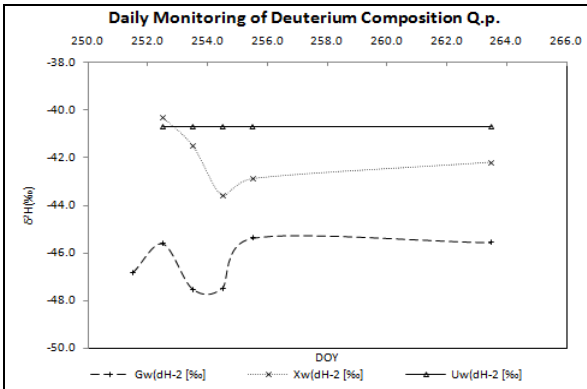

(c) 24hr groundwater and sapwater deuterium composition monitoring under Q.p.

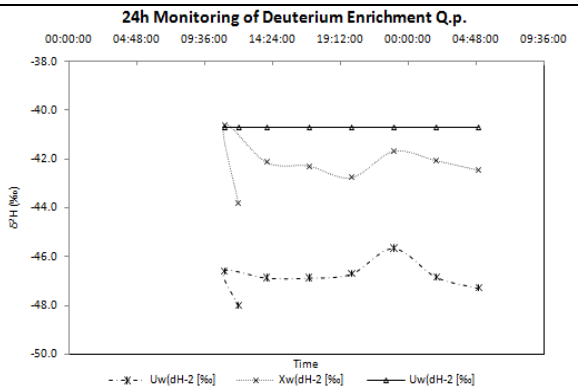

(d) daily groundwater and sapwater deuterium monitoring under Q.p.

Figure 29: Deuterium composition monitoring under ilex and *Q.p.*

The analysis showed that both species took water from the saturated and the unsaturated zones. The contribution from the groundwater to the transpiration process for *Q.i.* was 69% on average whilst for *Q.p.* was 76% on average. The 69% obtained in this study for *Q.i.* is close to 70% received by David et al. (2007). Hydraulic lift could be a possible source of immense influence on the above contribution from the groundwater (David et al., 2007).

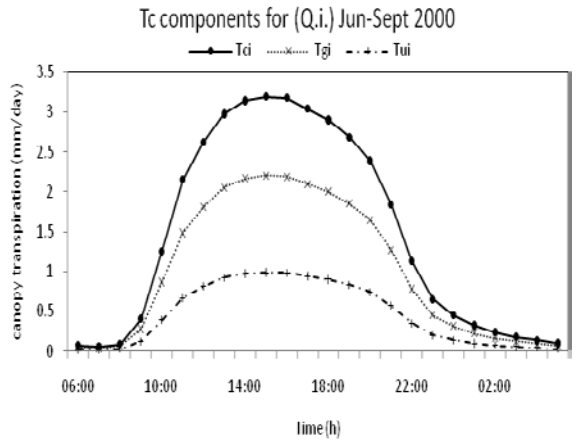

a) Transpiration components for Q.i.

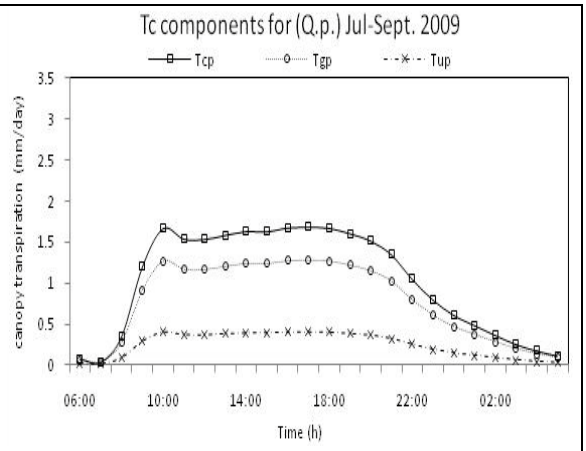

b) Transpiration components for Q.p.

Figure 30: Partition of transpiration into Tu and Tg

In Figure 29a, the canopy transpiration of *Q.i.* had been partitioned into the groundwater and unsaturated zone transpirations with a peak of 2.2 mm/day from the groundwater and the 0.99 mm/day from the unsaturated zone. The mean daily canopy transpiration component from groundwater for *Q.i.* was 1.01mm/day and from the unsaturated zone 0.46 mm/day. In the same way Figure 29b shows the partitioned canopy transpiration of *Q.p.* from the two zones with peak values of 1.26mm/day mm/day and 0.96mm/day for *Q.p.* The two zones contribute 0.78mm/day and 0.25 mm/day to the transpiration.

4.5. Spatial representation of Tg

4.5.1. Canopy groundwater transpiration

The distribution of the canopy groundwater transpiration (T_{cg}) of each species is represented in Figure 30, within the selected plot (Fig.1). The canopy groundwater transpiration within the catchment ranges from 0.014 – 0.507 mm/day and 0.019 – 0.615 mm/day for *Q.i.* and *Q.p.* respectively in the dry season 2009. The September 2009 values are lower than the mean dry season.

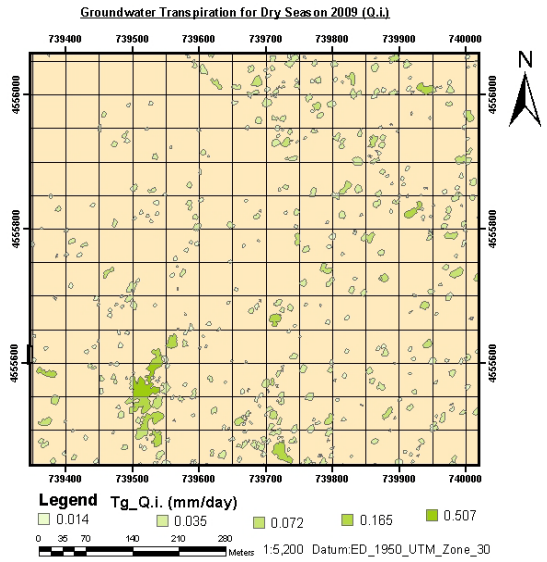

a) canopy groundwater transpiration in dry season 2009 (Q.i.)

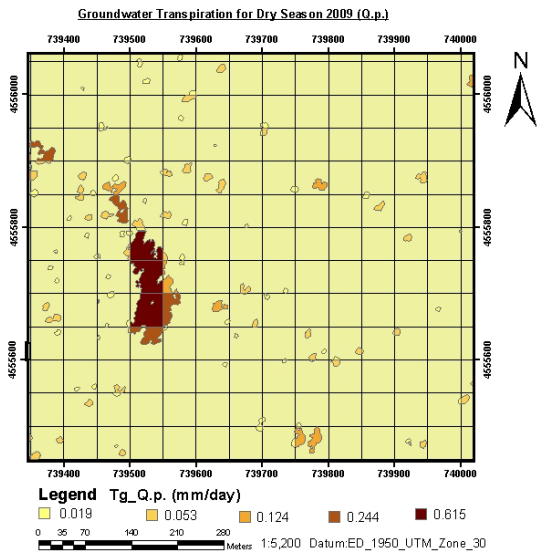

b) canopy groundwater transpiration in dry season 2009 (Q.p.)

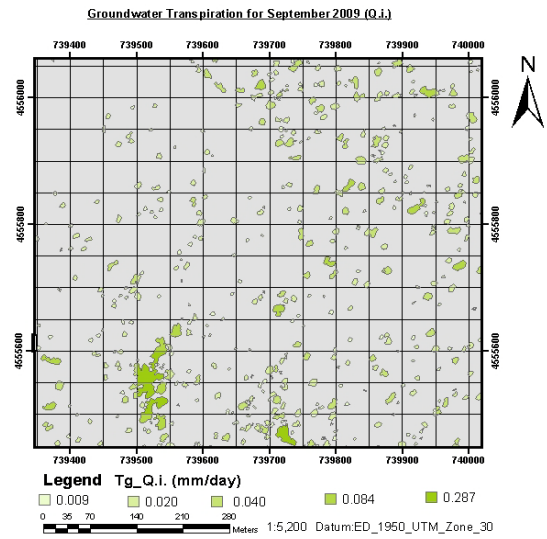

c) canopy groundwater transpiration in September 2009 (Q.i.)

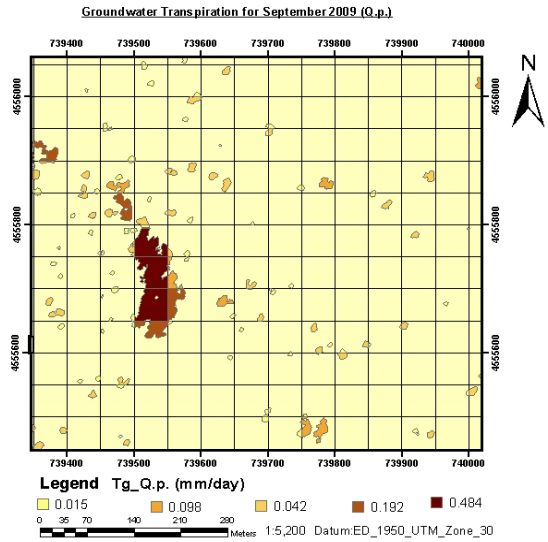

d) canopy groundwater transpiration in September 2009 (Q.p.)

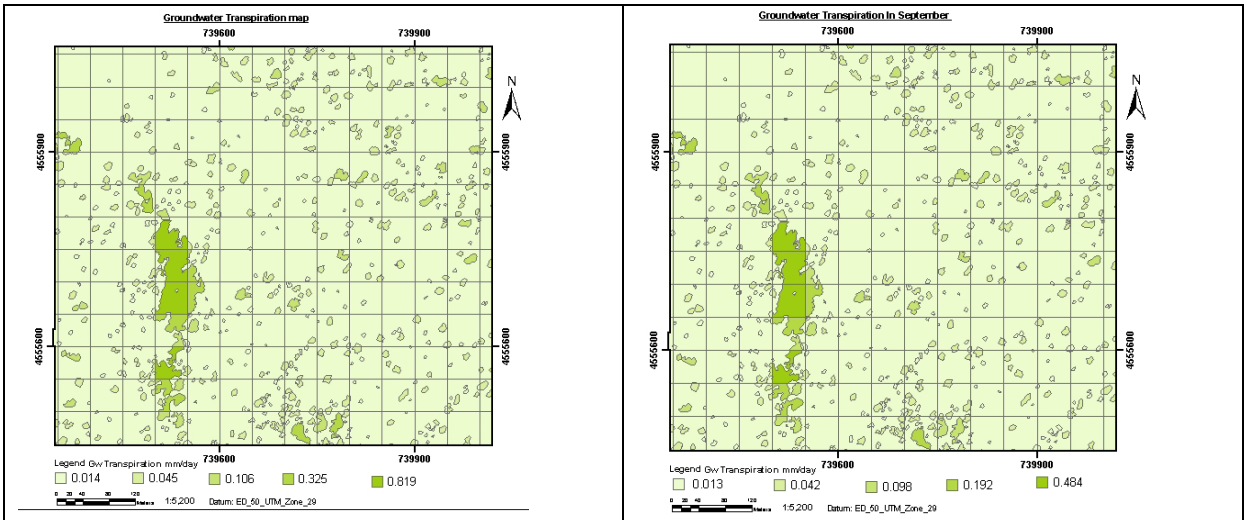

e) canopy groundwater transpiration in dry season 2009

c) canopy groundwater transpiration in September 2009

Figure 31: Canopy groundwater transpiration by Q.i. and Q.p. in the selected plot

4.5.2 Plot groundwater transpiration

The plot groundwater transpiration is shown in Figure 32 in which a plot size of 1 ha was used in normalizing the transpiration. The value of the ground water transpiration is between 0 – 0.022 mm/day for Q.i with a mean value of 0.001 mm/day in the dry season 2009. For Q.p. Tg is 0.015 – 0.391 mm/day with a mean value of 0.036 mm/day. In Figure 32 c groundwater transpition is 0.012 – 0.393 mm/day with a mean of 0.046 mm/day for the dry season 2009. In September, the value ranges 0.00 – 0.309 mm/day which is generally lower than for the period of the dry season

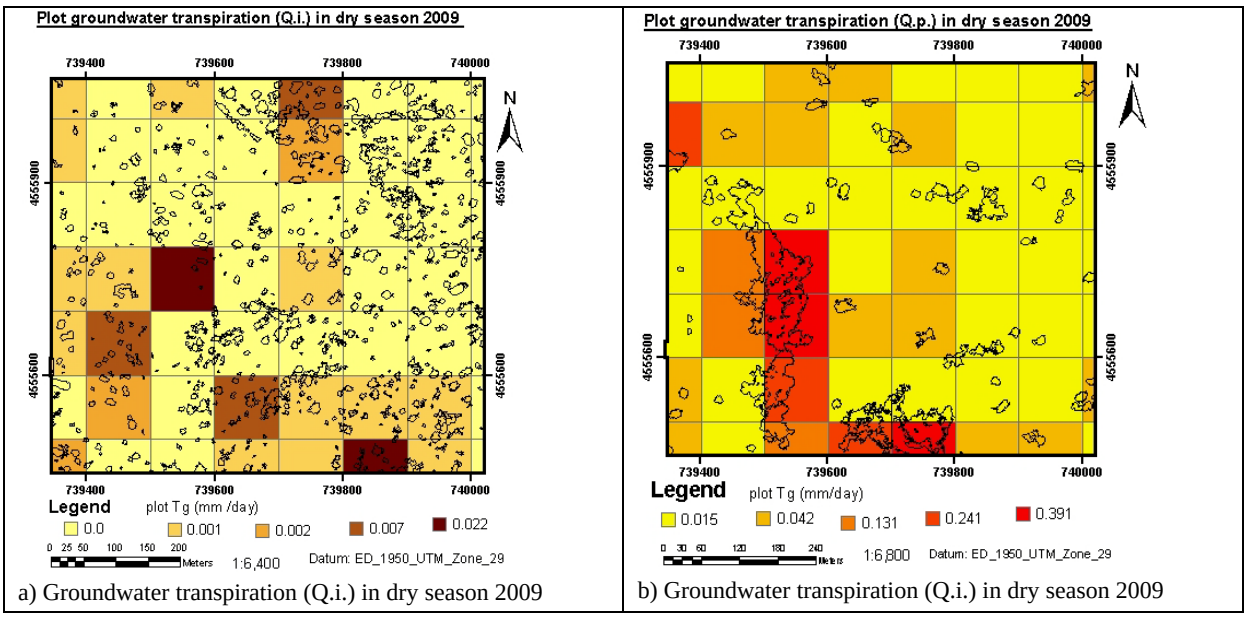

a) Groundwater transpiration (Q.i.) in dry season 2009

b) Groundwater transpiration (Q.i.) in dry season 2009

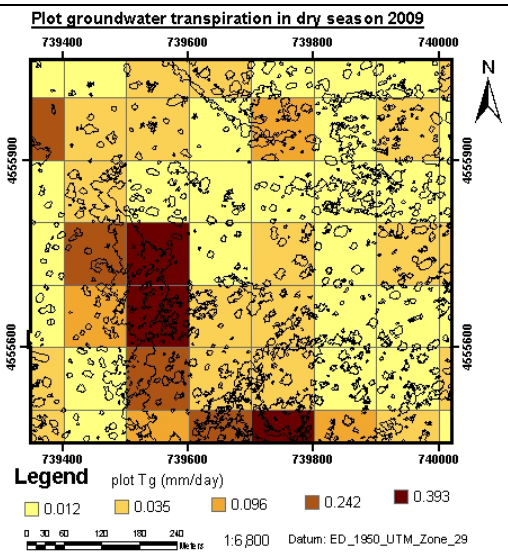

a) Groundwater transpiration (Q.i.) in dry season 2009

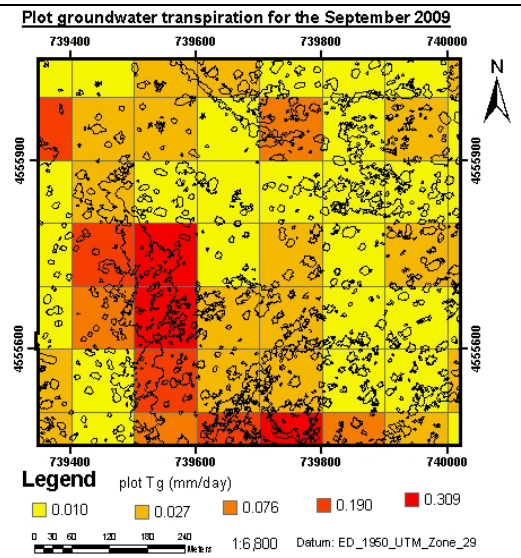

a) Groundwater transpiration (Q.i.) in dry season 2009

Figure 32: spatial distribution of plot groundwater transpiration in the dry season 2009

4.5.2. 4.5.3 Catchment groundwater transpiration

In Figure 33, the spatial distribution of transpiration computed based on the catchment with the values ranging from from 0.0004 – 0.0013 mm/day for the dry season 2009. In the same way, the plot transpiration for September is 0 – 0.0009 mm/day and the mean is 0.000012 mm/day. On the plot basis the values are quite lower in September.

5. Conclusion and Recommendation

5.1. Conclusion

Estimating tree groundwater transpiration has been the objective of this work. This has been achieved through all the various stages combining various methods. The use of transpiration measurement, groundwater and xylem-sap isotope monitoring and soil matric potential measurement were successful in evaluating the contribution from the groundwater to the transpiration process.

The conclusions drawn from this study are:
The assessment of transpiration in the catchment and partitioning to components from unsaturated and ground water throws light on sources of water for transpiration in the catchment. Groundwater plays a significant role in the transpiration process of the catchment. The dry season tree groundwater transpiration is above 60% of total tree trasnpiration. This is vital in analyzing role that groundwater plays in the transpiration.

There is always uncertainty in estimating the transpiration of a trees due to radial, circumferential and axial variation as the sap flux measured in different directions and positions around trees vary. However, as explained by Lu (Lu et al., 2000) the single measurement can be relied on *a priori* circumferential variation in a species, provided it accounts for radial variability of sap flux density.

Assessment of the radial variations of sap flux density in both species has given preliminary idea on radial profiles and will be further explored in the future estimations of sap flux density in each species to generalize them per species.

The heat field deformation method has been very good in assessment of radial variation of sap flux density. The radial variation in sap flux density with sapwood depth differs in *Q.i* and *Q.p.* As the flow is routed towards the outer xylem, for *Q.p.* it is mostly high while for *Q.i.* is high in the inner sap-wood.

Transpiration of the individual trees had been upscaled into the catchment level by using image retrieved canopy areas and by using biometric upscaling functions. The upscaling of transpiration using RS and GIS approach provides a good and efficient way to evaluate the spatial and eventually temporal distribution of the transpirations within the catchment.

The accuracy of the upscaled transpiration is limited by the accuracy of sap flux density measurement, xylem area measurement, BUF, species classification and canopy area delineation. A very high resolution image though expensive is the remedy for this.

The stable isotope method provides an efficient way of evaluating the water uptake sources for transpiration as the transpiration is partition into the unsaturated and groundwater transpiration effectively using stable isotope tracing and soil matric potential.

5.2. Recommendation

It is recommended that further study needs be carried out on additional tree sizes in the catchment for the relationship shown in sap flux - sapwood radial variation to establish and model with environmental factors in other to predict transpiration flux of *Q.p.* and *Q.i*

Further study needs to be conducted on *Q.p.* and *Q.i.* to confirm their phreatophryte characters and quantify their groundwater contributions with regard to their growing stage and in time.

The root depth and structure for each species should be evaluated using electrical resistivity method to determine in order to have a more dependable plot of the transpiration curve

Further studies should look at the hydraulic lift contribution to the amount of water transpired by each species and also capillary rise from the groundwater and study be conducted on whether any of the species is involved in hydraulic redistribution.

REFERENCES

Attanayake, A.N.B., 1999. Analysis of fractures in a granitic terrain and their tectonic and hydrogeological implications: a study from Sardon Catchment area, Salamanca Province, Spain. MSc. Thesis, ITC, Enschede, 61 pp.

Baird, K.J. and Maddock III, T., 2005. Simulating riparian evapotranspiration: a new methodology and application for groundwater models. Journal of Hydrology, 312(1-4): 176-190.

Brereton, J., Fitzgibbon, J., May, P. and Will, J., 2009. Tree handbook. Metropolitan Tree Growers Pty. Ltd, Melbourne.

Brunel, J.P., Walker, G.R., Dighton, J.C. and Monteny, B., 1997. Use of stable isotopes of water to determine the origin of water used by the vegetation and to partition evapotranspiration. A case study from HAPEX-Sahel. Journal of Hydrology, 188-189: 466-481.

Burgess, S.S.O., Adams, M.A. and Bleby, T.M., 2000a. Measurement of sap flow in roots of woody plants: a commentary. Tree Physiology 20: 909-913.

Burgess, S.S.O., Adams, M.A., Turner, N.C. and Ward, B., 2000b. Characterisation of hydrogen isotope profiles in an agroforestry system: implications for tracing water sources of trees. Agricultural Water Management, 45(3): 229-241.

Čermák, J., Kučera, J. and Nadezhdina, N., 2004. Sap flow measurements with some thermodynamic methods, flow integration within trees and scaling up from sample trees to entire forest stands. Trees - Structure and Function, 18(5): 529-546.

Chavarro-Rincón, D., 2009. Tree traanspiration mapping from upscaled sap flow in the Botwsana Kalahari. Dissertation Thesis, ITC, University of Twente, Enschede, 140 pp.

Corcuera, L., Camarero, J. and Gil-Pelegrín, E., 2004. Effects of a severe drought on Quercus ilex radial growth and xylem anatomy. Trees - Structure and Function, 18(1): 83-92.

Cramer, V.A., Thorburn, P.J. and Fraser, G.W., 1999. Transpiration and groundwater uptake from farm forest plots of Casuarina glauca and Eucalyptus camaldulensis in saline areas of southeast Queensland, Australia. Agricultural Water Management, 39(2-3): 187-204.

Cubera, E. and Moreno, G., 2007. Effect of single Quercus ilex trees upon spatial and seasonal changes in soil water content in dehesas of central western Spain. Ann. For. Sci., 64(3): 355-364.

David, T.S. et al., 2007. Water-use strategies in two co-occurring Mediterranean evergreen oaks: surviving the summer drought. Tree Physiology, 27: 793–803.

Dawson, T.E., 1996. Determining water use by trees and forests from isotopic, energy balance and transpiration analysys: the role of tree size and hydraulic lift. Tree Physiology, 16(3): 263-272.

Dawson, T.E., Mambelli, S., Plamboeck, A.H., Templer, P.H. and Tu, K.P., 2002. Stable isotopes in plant ecology. Annual Review of Ecology and Systematics, 33(1): 507-559.

Dingman, S.L., 2002. Physical Hydrology. Prentice hall , Upper Saddle River, New Jersey 07458, 646 pp.

Dongmei, W., Baohui, Z., Xingcheng, Z., Xilin, W. and XiaoyanC, W., 2004. Problem Identification and needs assessment of agricultural water resource management in China, ISCO 2004 - 13th International Soil Conservation Organisation Conference Brisbane, China.

Ehleringer, J.R. and Dawson, T.E., 1992. Water uptake by plants: perspectives from stable isotope composition. Plant, Cell and Environment, 15(9): 1073-1082.

Exploring the World of Trees, 2009 (access yr). Pyrenaica oak. <http://tree-species.blogspot.com/2008/11/pyrenean-oak-quercus-pyrenaica-melojo.html>.

FAO, 1995. Water sector policy review and strategy formulation. A general framework. FAO land and water bulletin - 3, Rome, Italy http://www.fao.org/docrep/v7890e/V7890E0b.htm.

Fetter, C.W., 2001. Applied hydrogeology. Pearson Education, Upper Saddle River, New Jersey 07458.

Gartner, K., Nadezhdina, N., Englisch, M., Cermak, J. and Leitgeb, E., 2009. Sap flow of birch and Norway spruce during the European heat and drought in summer 2003. Forest Ecology and Management, 258(5): 590-599.

González, L., 2001. Determination of Water Potential in Soils, Handbook of Plant Ecophysiology Techniques, pp. 213-222.

Gourbesville, P., 2008b. Integrated river basin management, ICT and DSS: Challenges and needs. Physics and Chemistry of the Earth, Parts A/B/C, 33(5): 312-321.
Granier, A., 1985. Une nouvelle methode pour la mesure dy flux de seve brute le trons des arbres. Ann. For. Sci., 22: 193-200.
Hernández-Santana, V., Martínez-Fernández, J., Morán, C. and Cano, A., 2008. Response of Quercus pyrenaica (melojo oak) to soil water deficit: a case study in Spain. European Journal of Forest Research, 127(5): 369-378.
ICT, 2009. Heat filed deformation sap flow. In: ICT international pty ltd (Editor), p.o. box 503 Armidale NSW 2350, Australia.
International Water Law Project, 1989. Charter on ground-water management as adopted by the Economic Commission for Europe at its fort-fourths session (1989) by decision E(44). In: N.Y. United Nations, 1989 (Editor).
Jin, X., 2009. Ecohydrology in water-limited environments using quantitative remote sensing - the Heihe River basin (China) case, Wageningen University, Wageningen, The Netherlands, 121 pp.
Kendall, C. and McDonnell, J.J. (Editors), 1998. Isotope tracers in catchment hydrology. Elsevier Science BV, Sara Burgerstraat 25, P.O. Box 211, 1000AE Armsterdam, The Netherlands, 839 pp.
Köstner, B., Granier, A. and Cermák, J., 1998. Sapflow measurements in forest stands: methods and uncertainties. Ann. For. Sci., 55(1-2): 13-27.
Lambs, L. and Berthelot, M., 2002. Monitoring of water from the underground to the tree: first results with a new sap extractor on a riparian woodland. Plant and Soil, 241(2): 197-207.
Lambs, L., Loudes, J.-P. and Berthelot, M., 2002. The use of the stable oxygen isotope to trace the distribution and uptake of water in riparian woodlands. Nukleonica, 47: 71-74.
Lamontagne, S., Cook, P.G., O'Grady, A. and Eamus, D., 2005. Groundwater use by vegetation in a tropical savanna riparian zone (Daly River, Australia). Journal of Hydrology 310(1-4): 280-293.
Lu, P., Müller, W.J. and Chacko, E.K., 2000. Spatial variations in xylem sap flux density in the trunk of orchard-grown, mature mango trees under changing soil water conditions. Tree Physiology, 20: 683-692.
Lu, P., Urban, L. and Zhao, P., 2004. Granier's thermal dissipation prope (TDP) method for measuring sap flow in trees: theory and practice. Acta Botanica Sinica, 46(6): 631-645.
Lubczynski, M., 2009. The hydrogeological role of trees in water-limited environments. Hydrogeology Journal, 17: 247-259.
Lubczynski, M.W. and Gurwin, J., 2005. Integration of various data sources for transient groundwater modeling with spatio-temporally variable fluxes--Sardon study case, Spain. Journal of Hydrology, 306(1-4): 71-96.
Mapanda, W., 2003. Scaling-up tree transpiration of eastern Kalahari sandveld of Botswana using remote sensing and geographical information systems. MSc. Thesis, ITC, Enschede, 70 pp.
Miller, G.R., 2009. Measuring and modeling interactions between groundwater, soil moisture, and plant transpiration in natural and agricultural ecosystems. Dissertation Thesis, University of California, Berkeley, USA, Berkeley, 243 pp.
Nadezhdina, N., Cermak, J. and Ceulemans, R., 2002. Radial patterns of sap flow in woody stems of dominant and understory species: scaling errors associated with positioning of sensors. Tree Physiol, 22(13): 907-918.
Nadezhdina, N., Cermak, J., Gasparek, J., Nadezhdin, V. and Prax, A., 2006. Vertical and horizontal water redistribution in Norway spruce (Picea abies) roots in the Moravian Upland. Tree Physiol, 26(10): 1277-1288.
Nadezhdina, N., Ferreira, M., Silva, R. and Pacheco, C., 2008. Seasonal variation of water uptake of a Quercus suber tree in Central Portugal. Plant and Soil, 305(1): 105-119.
Nadezhdina, N., Tributsch, H. and Čermák, J., 2004. Infra-red images of heat field around a linear heater and sap flow in stems of lime trees under natural and experimental conditions. Ann. For. Science, 61: 203 - 213
Ontiveros, E.R., 2009. Tree transpiration, a spatio-temporal approach in water limited environments: Sardon study case. MSc. Thesis, ITC, Enschede, 65 pp.

Oren, R., Phillips, N., Ewers, B.E., Pataki, D.E. and Megonigal, J.P., 1999. Sap-flux-scaled transpiration responses to light, vapor pressure deficit, and leaf area reduction in a flooded Taxodium distichum forest. Tree Physiology 19: 337--347.

Ridolfi, L., D'Odorico, P. and Laio, F., 2006. Effect of vegetation - water table feedbacks on the stability and resilience of plant ecosystems. Water Resour. Res., 42.

Salinas, A., 2010. A study case on the upscaling of tree transpiration in water limited environments. MSc. Thesis, ITC, University of Twenty, Enschede.

Schwinning, S., Davis, K., Richardson, L. and Ehleringer, J.R., 2002. Deuterium enriched irrigation indicates different forms of rain use in shrub/grass species of the Colorado Plateau. Oecologia, 130: 345-355.

Shakya, D.R., 2001. Spatial and temporal groundwater modeling integrated with RS and GIS : Hard rock experimental catchment Sardon, Spain. MSc. Thesis Thesis, ITC, Enschede, 97 pp.

Silva, J., Rego, F. and Martins-Louçao, M., 2003. Root distribution of Mediterranean woody plants. Introducing a new empirical model. Plant Biosystems, 137: 63-72.

Silva, J.S. and Rego, F.C., 2004. Root to shoot relationships in Mediterranean woody plants from Central Portugal. Biologia, Bratislava, 59/Suppl. 13(1).

Simmers, I. (Editor), 2003. Understanding water in a dry environment: hydrological processes in arid and semi-arid zones. International association of hydrogeologists, 23. A.A. Balkema Publisher, A member of Swets & Zeitlinger B.V., Lisse, The Netherlands, 337 pp.

Smith, D.M. and Allen, S.J., 1996. Measurement of sap flow in plant stems. J. Exp. Bot., 47(12): 1833-1844.

Snyder, K.A. and Williams, D.G., 2000. Water sources used by riparian trees varies among stream types on the San Pedro River, Arizona. Agricultural and Forest Meteorology, 105(1-3): 227-240.

Stromberg, J.C., Tiller, R. and Richter, B., 1996. Effects of Groundwater Decline on Riparian Vegetation of Semiarid Regions: The San Pedro, Arizona. Ecological Applications, 6(1): 113-131.

Tateishi, M. et al., 2008. Spatial variations in xylem sap flux density in evergreen oak trees with radial-porous wood: camparisons with anaomical observations. Tree 22(8): 23-30.

Teixeira, A.H.d.C., 2008. Measurements and modelling of evapotranspiration to asses agricultural water productivity in basins with changing land use patterns: A case study in São Francisco River basin, Brazil. Doctoral Thesis, Wageningen University, Wageningen, The Netherlands.

Tesfai, B.H., 2001. Subsurface characterisation of granitic basement from structural and resistivity data : a case study from Sardon Catchment area. MSc. Thesis, ITC, Enschede, 74 pp.

Thorburn, P.J., Hatton, T.J. and Walker, G.R., 1993. Combining measurements of transpiration and stable isotopes of water to determine groundwater discharge from forests. Journal of Hydrology, 150(2-4): 563-587.

Uria Cornejo, S.P., 2000. Groundwater recharge modelling in hard rocks: Sardone case study, Spain. MSc Thesis, ITC, Enschede, 89 pp.

Verbeeck, H. et al., 2007. Stored water use and transpiration in Scots pine: a modeling analysis with ANAFORE. Tree Physiol, 27(12): 1671-1685.

Walker, G. et al., 2001. The use of stable isotopes of water for deternining sources of water for plant transpiration, CSIRO Land and Water, SA 5064, Australia.

Wikipedia, 2009 -a. *Quercus ilex*. http://en.wikipedia.org/wiki/Quercus_ilex

Wikipedia, 2009 -b. *Quercus pyrenaica*. http://es.wikipedia.org/wiki/Quercus_pyrenaica.

Wullschleger, S.D. and King, A.W., 2000. Radial variation in sap velocity as a function of stem diameter and sapwood thickness in yellow-poplar trees. Tree Physiol, 20(8): 511-518.

Wullschleger, S.D. and Norby, R.J., 2001. Sap velocity and canopy transpiration in a sweetgum stand exposed to free-air CO2 enrichment (FACE). New Phyrologist 150: 489–498.

Ziegler, H., Weber, J. and Lüttge, U.E., 2009. Thermal dissipation probe measurements of sap flow in the xylem of trees documenting dynamic relations to variable transpiration given by instantaneous weather changes and the activities of a mistletoe xylem parasite. Trees, 23: 441–450.

5.3. Appendix

La Mata Catchment - Spain
Estimating Tree Groundwater Transpiration
Soil Matric Potential Data for PRY_7.1
19/09/2009

ID PYR 7	depth (cm)	Dist (m)	Mc (g)	Msoil (g)	ψ(Mpa)	ψ(pF)	T °C
SSM25-1	25	3.15	1.56	7.56	-9.12	4.93	21
SSM50-1	50	3.15	1.56	7.61	-7.18	4.87	21
SSM75-1	75	3.15	1.57	7.63	-1.22	4.10	21
SSM100-1	100	3.15	1.57	7.72	-0.62	3.80	21
SSM25-2	25	6.3	1.56	7.62	-10.27	5.03	21
SSM50-2	50	6.3	1.55	7.59	-11.33	5.07	21
SSM75-2	75	6.3	1.55	7.49	-6.01	4.80	21
SSM100-2	100	6.3	1.56	7.64	-0.42	3.82	21
SSM25-3	25	12.3	1.55	7.72	-6.99	4.86	21.27
SSM50-3	50	12.3	1.55	7.72	-1.78	4.25	21
SSM75-3	75	12.3	1.55	7.67	-0.46	3.67	21
SSM100-3	100	12.3	1.56	7.57	-0.02	2.14	21
NMS25-1	25	1.65	1.57	7.52	-2.92	4.47	21
NSM50-1	50	1.65	1.56	7.61	-1.32	4.06	21
NSM75-1	75	1.65	1.56	7.55	-0.39	3.58	21
NSM100-1	100	1.65	1.56	7.60	-0.47	3.62	22
NSM25-2	25	3.15	1.56	7.62	-4.55	4.67	21
NSM50-2	50	3.15	1.58	7.62	-0.56	3.68	21
NSM75-2	75	3.15	1.56	7.56	-0.46	3.60	21
NSM100-2	100	3.15	1.56	7.66	-0.16	3.20	22
NSM25-3	25	12.3	1.57	7.37	-8.08	4.92	21
NSM50-3	50	12.3	1.57	7.64	-1.39	4.16	21
NSM75-3	75	12.3	1.57	7.54	-0.35	3.50	21
NSM100-3	100	12.3	1.56	7.48	-0.09	3.00	21

Table 8: Results of Matric Potential Measurement for Q. Pyrenaica Using WP4

La Mata Catchment - Spain
Estimating Tree Groundwater Transpiration
Soil Matric Potential Data for ILEX_8.1
08/10/2009

ID	Depth (cm)	Dist (m)	Mc (g)	Msoil (g)	ψ(Mpa)	ψ(pF)	T °C
SSM25-1	25	1.55	1.56	7.57	-5.65	4.77	21
SSM50-1	50	1.55	1.56	7.67	-1.60	4.21	22
SSM75-1	75	1.55	1.56	7.52	-1.71	4.25	22
SSM100-1	100	1.55	1.56	7.62	-2.40	4.39	22
SSM25-2	25	3.15	1.57	7.65	-2.46	4.41	22
SSM50-2	50	3.15	1.57	7.69	-1.73	4.25	22
SSM75-2	75	3.15	1.56	7.70	-0.91	3.97	22
SSM90-2	90	3.15	1.56	7.59	-0.90	3.96	21
SSM25-3	25	5.15	1.57	7.70	-2.56	4.36	21
SSM50-3	50	5.15	1.56	7.54	-0.53	3.74	22
SSM75-3	75	5.15	1.56	7.71	-0.92	3.97	22
NSM25-1	25	1.9	1.56	7.46	-2.06	4.28	21
NSM50-1	50	1.9	1.57	7.36	-0.80	3.86	21
NSM75-1	75	1.9	1.56	7.66	-0.71	3.85	21
NSM100-1	100	1.9	1.56	7.76	-0.75	3.79	24
NSM25-2	25	3.8	1.57	7.87	-0.58	3.71	21
NSM50-2	50	3.8	1.56	7.05	-0.88	3.95	21
NSM75-2	75	3.8	1.56	7.59	-0.67	3.84	21
NSM100-2	100	3.8	1.56	7.04	-1.36	4.15	22
NSM25-3	25	9.8	1.56	7.40	-0.85	3.85	25
NSM50-3	50	9.8	1.56	7.62	-1.34	4.10	23
NSM75-3	75	9.8	1.56	7.03	-0.19	3.25	21
NSM-90-3	100	9.8	1.56	7.72	-0.50	3.69	21

Table 9: Results of Soil Matric Potential Measurement for Q. Ilex using WP4

La Mata Catchment - Spain
Estimating Tree Groundwater Transpiration
Soil Matric Potential Data for SEN_1.3
23/09/2009

ID SEN.1	Depth	Msoil (g)	ψ(Mpa)	ψ(pF)	T °C
St 25	25	7.148333	-3.79667	4.593333	21
St 50	50	7.273333	-0.96667	4	21
St 75	50	6.898333	-0.32333	3.52	21
St 100	100	7.356667	-0.18667	3.283333	21

Table 10: Result of Soil Matric potential measurement at bare area using WP4

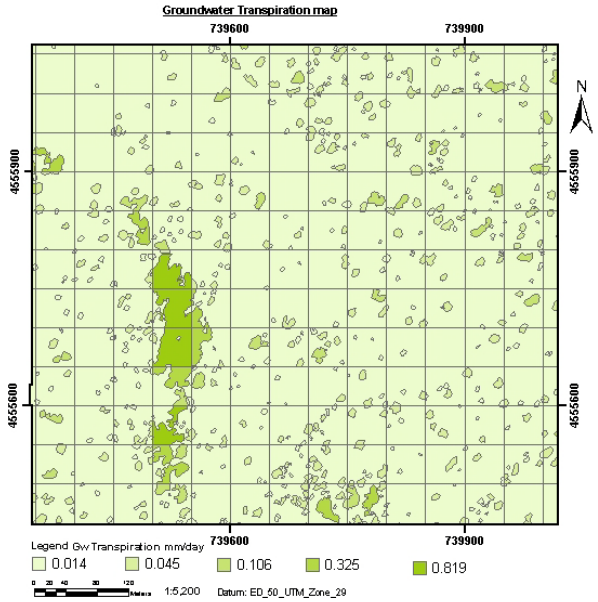

Figure 33: Mean groundwater transpiration from (June – Sept 2009)

Appendix B